Materials Today Chemistry 29 (2023) 101433

Contents lists available at ScienceDirect

Materials Today Chemistry

journal homepage: www.journals.elsevier.com/materials-today-chemistry/

Electropolymerized polypyrrole silver nanocomposite coatings on porous Ti substrates with enhanced corrosion and antibacterial behavior for biomedical applications

C. García-Cabezón [a, *], V. Godinho [b, **], C. Pérez-González [a], Y. Torres [b], F. Martín-Pedrosa [a]

[a] Departamento de Ciencia de Materiales y Ingeniería Metalúrgica, Escuela de Ingenierías Industriales, Universidad de Valladolid, Calle Paseo del Cace 59, 47011, Valladolid, Spain
[b] Departamento de Ingeniería y Ciencia de los Materiales y del Transporte, Escuela Politécnica Superior, Calle Virgen de África 7, 41011, Sevilla, Spain

ARTICLE INFO

Article history:
Received 18 August 2022
Received in revised form
25 December 2022
Accepted 3 February 2023
Available online 8 March 2023

Keywords:
Porous titanium
Corrosion behaviour
Biocompatibility
PPy-Ag composite coating
Conductive polymer
Nanostructures

ABSTRACT

This work proposes an innovative strategy that combines two well-known easy and economical preparation techniques: powder metallurgy based space-holder (SH) technique to provide porous biocompatible Ti substrates with balanced biomechanical behavior (for cortical bone tissue substitution) promoting bone ingrowth and biocoating infiltration, and electropolymerization to coat these substrates with the polypyrrole–silver nanoparticles (PPy-AgNPs) composite conductive polymers improving its corrosion resistance, biocompatibility with enhanced antibacterial activity. The deposited PPy-based coatings present a cauliflower-like structure well adhered to the porous substrates. The macroporosity of and rough inner pore surface of Ti SH substrates are responsible for the superior adhesion of the conductive polymer comparing to typical denser substrates obtained by powder metallurgy or forging. The corrosion protection properties of the coatings were investigated by open circuit potential and Anodic Polarization in PBS media to simulate possible implant conditions, revealing improved corrosion resistance for the composite coatings. The bioactivity of the coatings was evaluated by immersion tests, revealing the formation of Hydroxyapatite after 90-day immersion in PBS. In both PPy and PPy-AgNPs composite coatings, a displacement of the polarization curves to more noble potentials and a decrease in the current density, indicated that the coating's protective character is maintained after 90-day immersion in PBS. The antibacterial activity was assessed by using the Kirby–Bauer disk-diffusion method against *Staphylococcus aureus* (ATCC 25923). The inhibition halo increased from 5.5 ± 0.4 mm for the bare substrate to 8.2 ± 0.6 mm for the PPy-coated substrate and to 12.5 ± 0.7 mm for the PPy-AgNPs-coated porous Ti. This feature associated to the improved corrosion protection and biocompatibility would significantly contribute to the success of the potential use of porous Ti implants by SH technique envisaging substitution of small damaged bone tissues for example in tumors.

1. Introduction

Over the last decades, enormous efforts have been made in enhancing the mechanical and biological properties of metallic titanium implants. Particularly, recent advances in porous titanium produced by space-holder technique (SH) show these materials as very promising for implant applications [1,2]. The percentage and size of the porosity obtained with this technique depends on the spacer particles used. Adequate porosity must guarantee a good biomechanical (stiffness and yield strength) and biofunctional (bone in-growth and osseointegration) balance, which allows solving the problems of bone resorption and loosening of the implant, reducing the risk of failure/rejection of these [1–3]. Although it has been observed that porosity improves the activity of osteoblasts, they are also preferential sites for the proliferation of bacteria and corrosion phenomena.

It is known that titanium implants present excellent corrosion resistance associated with the formation of a protective TiO_2 layer; however, in the patient body, these implants are exposed to very corrosive environments. Highly oxygenated fluids and dissolved

* Corresponding author.
** Corresponding author.
E-mail addresses: crigar@uva.es (C. García-Cabezón), vfortio@us.es (V. Godinho).

https://doi.org/10.1016/j.mtchem.2023.101433

oxygen, the presence of inorganic anions (Cl^-, HPO_4^{2-}, HCO^{3-}) and cations (Na^+, K^+, Ca^+, Mg^{2+}) or even changes in the pH caused by unexpected diseases or infections, together with the concentration of mechanical efforts over a highly porous material with rough and irregular pores, could seriously damage this protective layer, leading to the implant's corrosion [4–8]. The need to face these situations and to control any possible degradation drives the attention over polymeric protective coatings that can at the same time offer resistance against aggressive media, favor osseointegration, and even work as local therapeutic agent delivery [9,10].

In the field of corrosion protection, conductive polymer coatings have been widely investigated as they present high stability, high conductivity and provide protection of anodic dissolution, mediation of oxygen reduction and act as barriers and inhibitors [11–13]. Although the mechanism of protection of conductive polymers is not fully understood, investigations point out that the advantage of conductive polymers over other coatings is that they act not only as a physical barrier but also as an electronic barrier, which enhances the corrosion protection when compared to other materials that act only as physical barriers. One of the most investigated conductive polymers for corrosion protection of metals is polypyrrole (PPy), a biocompatible polymer [14,15] that can be electrosynthesized directly onto metallic implants [14]. Electropolymerization is a well-known technique to prepare conductive polymer coatings on different metals. The simplicity of the methodology, the control over the coatings thickness, the possibility for doping during synthesis and to perform in situ characterization of the polymer during its growth by electrochemical or spectroscopic methods are some of the advantages of this technique. This could be a very interesting and adequate procedure to coat highly porous small metallic implants produced by SH technique, the size of the pores produced favors the introduction of the electrolyte solution, and its irregular pore shape and roughness could further improve the adhesion of the coating to the substrates as previously observed for coatings of different nature, including polymeric coatings [16–19].

It has been reported that the protective effect of PPy coatings on stainless steel by a mixed mechanism of isolation and load transfer, displacing the corrosion potential to more positive values and reducing the corrosion current [20–22]. Another protection mechanism is based on anion exchange stabilizing the formation of a passive layer at the metal surface [21,23]. Moreover, the redox behavior of PPy was found to provide self-healing properties to scratched coatings [23,24] this could be of great interest in the case of biocoatings subjected to concentration of mechanical efforts in aggressive environments. Recently, PPy was successfully applied to the protection of porous stainless-steel substrates obtained by powder metallurgy (PM) [25]. These are however substrates with low porosity (around 10%) when compared to those obtained by SH. In the present work, PPy films are prepared by electrodeposition directly on highly porous Ti-cp substrates by SH technique, aiming to improve the corrosion resistance of potential candidates for small bone implants.

A first step limiting the functionality of the protective coatings is the adherence; previous works have reported lack of adhesion of PPy to oxidizable metals [8]. Recently, electopolymerized PPy coatings were successfully deposited on porous stainless-steels substrates, claiming that porosity is improving the adhesion of PPy to the metallic surfaces [25,26]. Following this late work, a highly porous surface of Ti substrates would favor the adhesion of the conductive PPy coatings.

PPy has been reported to not only to be biocompatible but also to favor cell adhesion and proliferation [27,28] as well as to have bactericidal activity [13,27]. Thus, the association of PPy bioprotective coatings with SH porous Ti substrates would provide not only the adequate mechanical properties with biofunctional balance (corrosion resistance and bone ingrowth) for example in the replacement of small, damaged bone tissues but also would work as antibacterial layer. A relevant challenge to a successful implant is the mitigation and prevention of the high rate of implant-related infections, a protective conductive polymer layer with antibacterial activity could make a difference being an alternative to traditional administration of antibiotics. The antibacterial activity of PPy has been attributed to a strong electrostatic interaction between the polymer structure, positively charged, and the bacterial cell walls that are negatively charged [13,28], destroying the bacterial cell wall, interacting with the cell membranes, disrupting the balance of proton transfer, and inhibiting the cellular respiration causing cell death [28].

It is also known that PPy can be doped with organic or inorganic materials during electropolymerization to improve hydrophobicity, corrosion resistance, adhesion, within others [26,29], and also with different drugs either antibiotics or anti-inflammatory to reduce fever and pain in biomedical applications [30,31]. Also, composites based on PPy nanoparticles with antibacterial agents such as Ag, CuO, or chitosan nanoparticles have been reported to show enhanced antibacterial activity [32–35]. In this work, we will focus on the introduction of a small amount of silver nanoparticles to produce PPy-protective composite coatings. Silver nanoparticles (AgNPs) have been described to damage bacterial cell via prolonged delivery of Ag + ions, showing a potent antimicrobial activity [36] and a low cytotoxicity [37], having better physiochemical and biological properties beyond bulk silver [38]. Even though concerns on adverse effects of silver nanoparticles in human have motivated different studies in the field of toxicity of silver nanoparticles [39,40] the discussion points that it is related to the size, shape, concentration, synthesis process, surface charge or coatings of the NPs [41]; the benefits of adding AgNPs in medical devices are known [42–44] particularly the application of nanoparticles as a drug to combat bacterial diseases either in a synergic effect enhancing the effectiveness of antibiotics [45–47] or as an alternative to the use of conventional antibiotics, avoiding the worldwide problem of antibiotic resistance [48]. In the present work, a small concentration of AgNPs was used, embedded in a PPy coating that will not degrade in the human body releasing the NPs. In this sense, we could take part of the benefits of the antibacterial effects silver nanoparticles allied to the ones of the PPy coating. Previous studies indicate that PPy-AgNPs composites with low concentration of AgNPs exhibits low cytotoxicity [35,49] balancing biocompatibility and antibacterial activity.

Moreover, in this work, we present an innovative approach by introducing PPy-based coatings as a strategy to enhance the corrosion resistance of highly porous Ti substrates prepared by SH technique to be used in small bone implant applications (as in the case of the need of substitution of damaged bone tissues as for example in bone tumors). Such combination of biopolymeric PPy-based material, loaded with silver nanoparticles, which allows at the same time, to improve the resistance to corrosion and to reduce the proliferation of bacteria; and porous titanium substrates (to solve the stress shielding phenomenon), was not, up to our knowledge, previously reported. The main idea is to explore further the properties of PPy-based coatings by putting together two well-known and easy and economical preparation techniques as PM-based SH technique to fabricate the implant substrate and electropolymerization to coat. Moreover, we investigate the roll of the PPy-protective layer on Ti porous substrates on the corrosion resistance in physiological environments as well as the antibacterial activity against staphylococcus aureus bacteria, a bacterium highly tolerant to saline environment. The different porosity, handily provided by SH technique, will allow to investigate the anticorrosion protective role of PPy coatings checking whether

there is a critical porosity limiting the protection of these coatings. For improving the antibacterial properties of these coatings, silver nanoparticles were added during electropolymerization. Wu and coworkers [35] have also investigated the incorporation of silver nanoparticles in electropolymerized PPy coatings. In their work, Ag nanoparticles were introduced via plasma immersion implantation. Up to our knowledge, no previous similar investigations have been published combining electropolymerized PPy and composites of PPy with silver nanoparticles deposited directly on porous Ti metallic substrates. Also, biological tests were included to further support the possibility to use the protected porous Ti substrates as implants. Moreover, the electrodeposition of composite PPy conductive polymers modified with metal nanoparticles could be off great interest for other potential applications, as in the case of electrochemical sensors, due to the high relation surface/volume, increasing the interest in these kind of composite materials [50,51].

2. Materials and methods

2.1. Fabrication and basic characterization of the porous Ti substrates

Porous Ti disks of 12 mm diameter, with different percentage of porosity, were prepared by SH technique. For this purpose, different amounts of ammonium bicarbonate(AB; 30–60 vol.%) with a size ranging from 250 to 355 μm were mixed with cp-Ti powders grade IV (SEJONG Materials Co. Ltd. Seoul, Korea), with a mean particle size (d_{50}) of 23.3 μm, in a Turbula T2C Shaker-Mixer for 40 min to ensure a good homogenization. Green substrates were obtained by pressing the mixtures in a universal Instron 5505 testing machine at 800 MPa. The AB spacers were thermally removed by heat treating the substrates in two stages of 12 h at 60 and 110 °C, under low vacuum condition of 10^{-2}mbar. A final step of sintering was carried out in a molybdenum chamber furnace (Termolab, Águeda, Portugal), for 2 h at 1250 °C under high-vacuum conditions (~10^{-5}mbar). More details on substrates' preparation and characterization can be found in Ref. [52]. On the other hand, for comparison purposes, in this work, coatings over commercial titanium substrates obtained by forging processes (cold rolling) and by conventional powder metallurgical routes (1300 MPa, sintering at 1300 °C, for 2 h and similar vacuum conditions) were evaluated.

In relation to the titanium substrates, in this work, a basic microstructural and mechanical characterization is carried out to verify the repeatability of the manufacturing process, comparing the results with previous ones by the authors. The porosity of the substrates was characterized by Archimedes and image analysis to evaluate the total porosity, interconnected porosity as well as the equivalent diameter. Scanning electron and confocal laser microscopies were used to assess the surface roughness. The stiffness and yield strength of the porous substrates were estimated following fitting equations described in the literature [53,54].

2.2. Electrodeposition of polypyrrole and PPy-Ag NPs composite coatings

Electropolymerization technique was used to obtain the coatings directly on the porous metallic substrates. It was carried out on an EG&G Parstat 273 A potentiostat/galvanostat at room temperature, with the classic three-electrode configuration. A platinum plate was used as counter electrode, the Ag/AgCl electrode in a 3 mol/L KCl solution as reference electrode, and, as working electrode, the Ti substrates with a final surface finishing polished with 1 μm diamond aqueous suspension and cleaned in an ultrasonic bath with water-ethanol.

To prepare the PPy coatings, we started from optimized conditions previously described for porous SS substrates [25,26]. The PPy coatings in the present work were obtained by electropolymerization at a constant potential of $0.9V_{Ag/AgCl}$ during 1800s, from a solution containing 0.1 mol/L of pyrrole and 0.05 mol/L of DBSA (Dodecylbenzene sulfonic acid) as dopant.

The synthesis of silver nanoparticle (AgNPs) colloids was carried out according to the procedure proposed by Creighton [55]. Two solutions were prepared: (1) $AgNO_3$ ($1 \cdot 10^{-3}$ mol/L) in deionized water and (2) $NaBH_4$ ($2 \cdot 10^{-3}$ mol/L) in deionized water; 30 mL of solution (2) with excess of ice-cold was placed on a stirring plate, then 10 mL of solution (1) was added drop by drop to the $NaBH_4$ solution with vigorous shaking to aid monodispersity. Using this procedure, a yellow colloid with a UV absorbance maximum at $\lambda = 393$ nm was obtained (Fig. S1a). Also, transmission electron microscopy measurements were performed to confirm size and crystallinity of the NPs, using a JEM 1011HR transmission electron microscope (JEOL USA, Inc., Peabody, MA) (Fig. S1b shows representative particle micrograph and electron diffraction).

PPy-AgNPs nanocomposites were synthesized by the 'trapping method' [50] from a solution containing 0.2 mol/L pyrrole and 0.1 mol/L DSA. This solution was mixed (1:1) with a solution containing AgNPs previously formed (Ag colloidal suspension). The electropolymerized films were obtained by chronoamperometry using a constant potential at 0.9 $V_{Ag/AgCl}$ over a period of 1800 s.

All samples were named as described in Table 1: first by the condition of the substrate, followed by PPy for polypyrrole coatings and by PPy/AgNPs for the case of the composite coatings.

2.3. Physicochemical and microstructural characterization of the coatings

The morphology, composition, and crystalline structure of the PPy and PPy-AgNPs coatings were investigated by scanning electron microscopy attached with energy-dispersive X-ray (SEM-EDX), attenuated total reflectance Fourier transform infrared spectrometry (ATR-FTIR) using an Cypher ES Spectrometer (Asylum Research, Santa Barbara, USA) and by X-ray diffraction (XRD) performed in an Agilent SuperNova diffractometer (Agilent Technologies XRD Products, Yarnton, UK) using micro CuKα/MoKα radiation with CCD Atlas detector (AgilentTechnologies XRD Products, OX5 1QU, UK). X-ray diffraction measurements were performed on coated Ti substrates and also on self-supported coatings that were peeled from the forged and conventional PM substrates to avoid the high intensity of substrate diffraction peaks. The morphology of the coatings was investigated by SEM (ESEM QUANTA 200 FEG, FEI, Hillsboro, OR, USA), and the average surface roughness (Ra) was studied by atomic force microscopy (AFM) measurements (CYPHER-ES Asylum Research, Santa Barbara, USA). Line scans as well as 2D and 3D images were obtained.

The study of the tribomechanical behavior of the coatings includes microhardness and adhesion resistance tests. The adhesion of the coatings to the Ti porous substrates was tested according to the ASTM D 4541–2 test method A [56] using Scoth Magic™ double-side tape, and a Mecmesin (BFG 50 N) dynamometer was used for evaluating the pull-off strength of the coatings, while that the hardness of coated substrates was evaluated, in a Matstusawa Microindenter, by performing Vickers microhardness tests using a load of 0.2 Kg and dwell time of 15 s. Also, small loads of 0.05 Kg were performed to evaluate the hardness of the coatings with lower influence of the substrate. The results obtained correspond to the arithmetic mean value of at least 10 indentations; the highest and lowest values were discarded.

Also, the conductivity of the PPy films at room temperature was evaluated through four-probe method using an HAAMEG HM

Table 1
Preparation routes and nomenclature of the samples in this work.

Bare substrates		Coated with polypyrrole (PPy)	Coated with polypyrrole + AgNPs (PPy/AgNPs)
Forged		Forged PPy	Forged PPy/AgNPs
PM 0 vol.%		PM 0 vol.%−Ppy	PM 0 vol.% - PPy/AgNPs
SH	30 vol.%	30 vol.% -PPy	30 vol.%- PPy/AgNPs
	40 vol.%	40 vol.% −Ppy	40 vol.%- PPy/AgNPs
	50 vol.%	50 vol.% −Ppy	50 vol.%- PPy/AgNPs
	60 vol.%	60 vol.% −PPy	60 vol.% -PPy/AgNPs

8040−2 I−V source meter, over the 12 mm disks by placing the probes equidistant.

2.4. Electrochemical corrosion measurements

Electrochemical corrosion measurements were carried out to test the behavior of the PPy-based coatings. To simulate a possible implant scenario, the tests were performed using PBS solution (0.8 g/L NaCl, 0.2 g/L KCl, 0.594 g/L Na_2HPO_4, 0.2 g/L KH_2PO_4) at a temperature of 37 °C ± 1 °C. The corrosion tests were carried out in a three-electrode conventional cell using a saturated calomel electrode (SCE) as the reference electrode and graphite as the counter-electrode. The test was performed in deoxygenated conditions (purged with nitrogen).

The open circuit potential was measured for 3600 s of immersion of the samples in the electrolyte solution. Potentiodynamic anodic potential curves were made following the ASTM G-5 [57]. After 30 min of open-circuit conditioning, the anodic potentiodynamic scan started at 50 mV below V_{OCP}, reaching 1000 mV_{SCE}, using 50 mV/min as the potential scan rate.

The corrosion rate was determined using Tafel's extrapolation methods. Tafel's cathodic and anodic slopes, the corrosion potentials, and the corrosion current densities were estimated from the Tafel plots. All tests were repeated three times for each condition.

EIS measurement was performed at open circuit potential from 10 MHz to 0.1 Hz at 10 data cycles/decade after measurement of the free potential from the immersion time during 1800s. All electrochemical experiments were repeated three times to verify reproducibility.

2.5. In vitro tests: bioactivity and antibacterial behavior

To investigate the biocompatibility of the coatings, immersion tests in PBS were performed during 90 days at 37 °C. After the immersion test, the formation of hydroxyapatite (HA) on the coatings was assessed by SEM-EDX.

The stability of the coatings after the biological test was also evaluated by anodic polarization (AP) tests after 90 days of immersion. In order to know which phases were dissolved after the corrosion process and to keep the piece in the same medium for 90 days, inductive coupling plasma with optical emission spectrophotometer (ICP-OES) was performed in a Perkin Elmer Optima 2000DV. The samples were measured directly, undiluted. The ICP equipment was calibrated with the following standards: 0, 0.01, 0.05, 0.1, 0.5, 1, and 10 ppm.

The antibacterial activity of the coatings was assed following the Kirby−Bauer disk-diffusion method [58] against *Staphylococcus aureus* (ATCC 25923) as bacterial model. Petri dishes containing Mueller−Hinton medium were covered with a suspension of bacteria (104 CFU/mL) using a sterile hyssop and the Ti substrates with the PPy-based coatings were placed on top of the seeded medium. Samples were incubated at 37 °C for 24 h in aerobic conditions. Inhibition halos were measured using ImageJ software. For statistical analysis, at least three measurements were performed for the different discs, and the results are expressed as the mean value and standard deviation. The statistical test used was a two-way ANOVA and Tukey's post-test (SPSS v. 22.0 for Windows, IBM Corp., Ar-monk, NY, USA). All determinations were analyzed in triplicate; $p < 0.05$ was considered statistical difference.

3. Results and discussion

3.1. Characterization of the porous Ti substrates

In previous works, we have explored the preparation conditions using different SH with different particle size and volume fraction to originate porous Ti implants with an appropriate balance between porosity that favors osseointegration and the resulting biomechanical properties, more details can be found in Refs. [2,59,60]. The purpose of the present work is to explore the protection effects against corrosion of conductive PPy coatings prepared by electropolymerization directly on the porous Ti substrates. In this sense, to explore both the possibility to prepare highly conformal coatings that could penetrate in the pores of such porous substrates, and the effectiveness of its corrosion resistance enhancement for the different degrees of porosity, we have deposited the polymeric coatings on substrates prepared with different degrees of porosity checking if there is a critical porosity limiting the protection of these coatings.

In the context of corrosion protection, the adhesion of the protective coatings to the metallic substrates is critical. Recent works show the improved adhesion of electropolymerized PPy to porous substrates [25,26].

Following these late works, a highly porous surface of Ti substrates would favor the adhesion of the conductive PPy coatings. Fig. 1 shows a comparison by SEM microscopy, between a Ti substrate prepared by PM (Fig. 1a) and a representative highly porous Ti substrate prepared with 50 vol.% of SH (Fig. 1b). All SH substrates presented similar pore size and morphology determined by the selected spacer corroborating the reproducibility of our previously reported results [33−35](check Table S1 for more information). Apart from small pores (around 10 μm) inherent to the typical PM procedure (as those in the PM substrate of Fig. 1a), the porous 50 vol.% substrate (Fig. 1b) presents large pores >200 μm that will allow the infiltration of the biopolymer. On the SEM images of the porous Ti substrate, the rough surface of the pores can be appreciated. Two levels of roughness are observed as shown in the images with different magnification (Fig. 1 b2 and b3). Also, the flat surface between the pores presents a certain roughness as it can be appreciated (Fig. 1 b1).

The percentage, size, and roughness of the walls of the macropores obtained in this work using the spacer technique allow to potentially guarantee the biomechanical balance (stiffness and yield strength) and biofunction (bone in-growth adhesion and proliferation of osteoblasts [1,2,61−63]), which requires the bone tissues that are intended to be replaced [64−66] and at the same

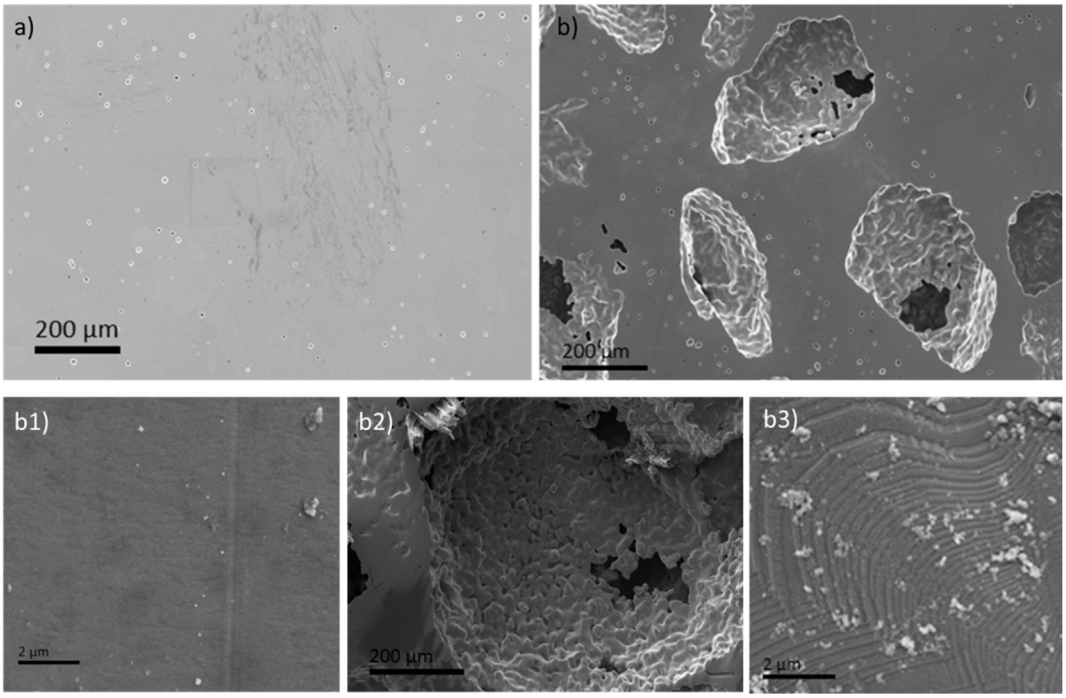

Fig. 1. Scanning electron micrographs of the Ti substrates (a) powder metallurgy substrate (0 vol.%), (b) porous 50 vol.% substrate. (b1) Detail of the flat surface between pores, (b2) detail of the inner pore surface, (b3) higher magnification of the pore surface.

time have an adequate size for the polymer infiltration and a surface roughness (inner and out of the pores) that would favor its adhesion to the metallic Ti substrates [67].

However, the irregular shape of these pores could also be not only a preferential site for the anchoring and proliferation of bacteria but also could determine the susceptibility of the implant material to localized corrosion when exposed to body fluids. Hence, the use of a biocompatible coating, with bactericidal activity, such as PPy could improve the implant success.

3.2. Electrodeposition and characterization of the polypyrrole coatings

The direct electropolymerization of the PPy and PPy-AgNps coatings on the porous metallic Ti substrates was successfully achieved, resulting in the formation of polymer coatings in all substrates. Fig. 2 shows the evolution of current density over time during electropolymerization of the PPy and PPy-AgNPs films using chronoamperometry. The curves in Fig. 2a present three typical features corresponding to the electropolymerization process: after a first period where the current density is low, due to the fact that the Ti surface is oxidized and diffusion controls the monomer oxidation; follows a second step where the current density increases rapidly with time corresponding to the nucleation and growth of the polymer on the Ti substrates [68]. Third, the current intensity reaches a plateau related to a progressive and continuous growth of the polymer coating thickness over time [14,69,70].

In this process, a clear beneficial influence of the substrate porosity can be observed, PPy electrodeposition over the denser forged and PM substrates present the lowest current density. This

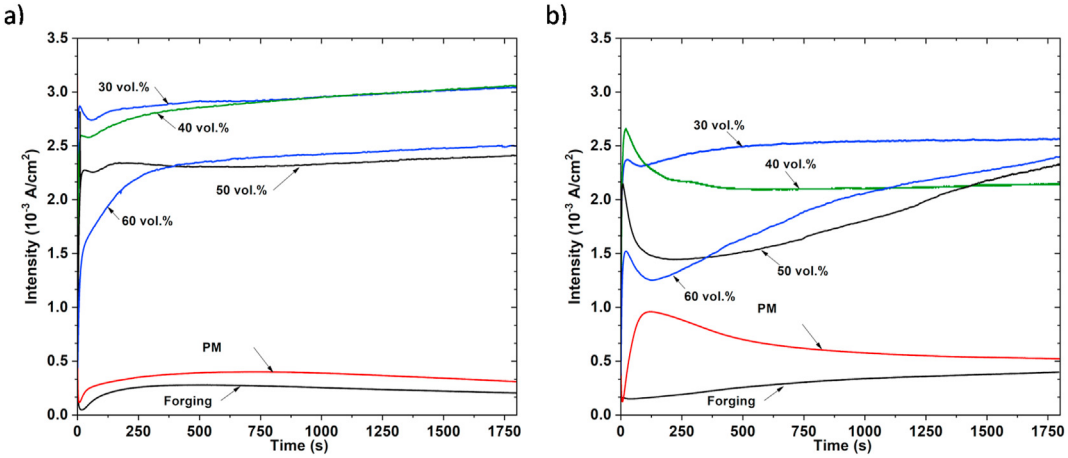

Fig. 2. Chronoamperograms at 0.9 V on the Ti substrates (a) polypyrrole (PPy) and (b) PPy-AgNPs.

implies that these substrates are exposed to lower current densities that can affect the adhesion of the polymer coatings and its growth.

In the case of the porous samples, differences are observed between the different degrees of porosity. The electrodeposition of PPy over the substrates prepared with 30% and 40% of SH presents higher current density, while for highly porous substrates, the electropolymerization current decreases, most probably due an increase of the effective area to be covered under the same deposition conditions. The increase of porosity for up to 60%vol. will also result in different surface morphology and chemical conditions (higher surface oxidation). This will strongly affect the quality and properties of the conductive polymeric coatings as it will be discussed in more detail in the next sections.

For the electrodeposition of the PPy-AgNPs composite coatings, a similar behavior to the previously described for PPy coatings was observed. The curves in Fig. 2b present similar stepped shape and the electrodeposition current densities increase with the increase of porosity up to 40 vol.%, decreasing for the highly porous substrates (50% and 60 vol.%). Comparing the current densities for both type of PPy-based coatings (PPy and PPy-AgNPs composite coatings), lower electrodeposition currents are achieved when silver NPs are added, showing that the Ag NPs are modifying the electropolymerization process, a discussion on the effects of the addition of nanomaterials into PPy matrix can be found in Ref. [29].

Fig. 3 presents the ATR-FTIR spectra of the coated Ti substrates (a) with PPy and (b)PPy/AgNPs composite coatings. In both spectra, features of PPy and DBSA can be observed [71,72]: a broad peak at 3400 cm^{-1} that can be associated to stretching modes of C—N from PPy, bands at 2959 cm^{-1}, and 2930 cm^{-1} corresponding to stretching of C—H either from DBSA or from the polymer and a peak at 2853 cm^{-1} corresponding to the aromatic C—H stretching vibrations. Characteristic peaks of PPy can be observed at 1590 cm^{-1}, 1558 cm^{-1}, and 1454 cm^{-1} associated to the fundamental vibrations of C═C and C—C of the protonated pyrrole ring. The wide and low-intensity band at 1289 cm^{-1} corresponds to in-plane vibration of C═C—N. The peaks at 1165 cm^{-1} and 1123 cm^{-1} correspond to vibrations of C—N and C—H in-plane aromatic stretching vibrations from the polymer and the dopant. At 1031 cm^{-1}, an intense band is observed attributed to bending modes of aromatic C—H, and a less intense band can be observed at 1006 cm^{-1} corresponding to S═O from the dopant. At 667 cm^{-1}, another band can be attributed both to the rocking vibration of C—H from the polymer and to the group SO_4. Peaks at 908 cm^{-1} and 797 cm^{-1} are attributed to the ring deformation and to the oscillation of the C—H vibrations, respectively.

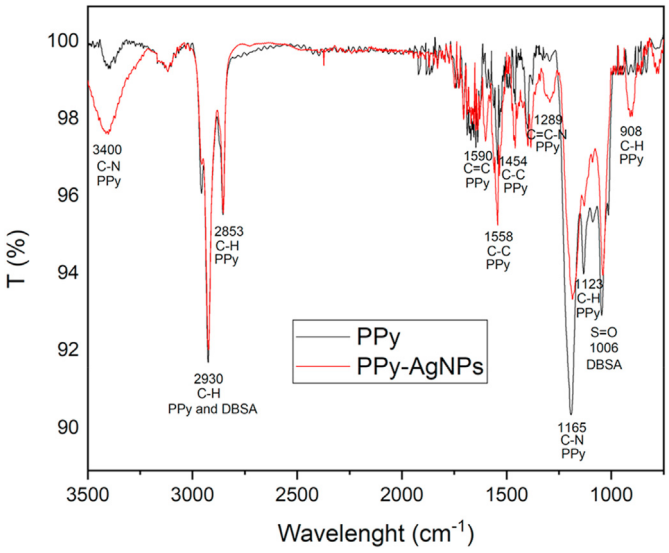

Fig. 3. ATR-FTIR spectra of PPy and PPy-AgNPs composite coatings.

As previously reported [73,74] PPy and PPy-Ag composite spectra are very similar; however, a certain displacement of peaks to lower wavenumber as well as differences in the relative intensities of peaks on the region from 1600 cm^{-1} to 1000 cm^{-1} that could be due to the compound interaction between the PPy and the silver nanoparticles [75].

The microstructure of these coatings was investigated by X-ray diffraction measured in Bragg—Brentano configuration in 2θ angles between 5 and 70°. Fig. 4 shows representative diffraction pattern of the coatings. The diffraction corresponding to the coated Ti substrate presents very intense peaks of Ti alfa (main peaks identified at 35.2, 38.4, 40.2, 53.0, 63.0, 70.5, 74.4, 76.3, 77.4, and 86.5°) and also a wide shoulder at small 2θ angles. To isolate the peaks from the thinner coatings from and those of the thick substrates and better appreciate the diffraction pattern of the PPy and PPy-AgNPs coatings, those were removed (pealed) from the denser substrates (forged Ti and conventional PM Ti substrates) and the self-supported coatings were measured. The XRD measurements revealed the amorphous structure of the PPy coatings as shown in Fig. 4 corresponding to a wide shoulder. In the case of the composite PPy-AgNPs coatings, peaks at 2θ angles of 38.1, 44.3, and 64.6° are observed and correspond to crystalline silver NPs [76].

SEM micrographs, Fig. 5, revealed the morphology of the coatings, a typical PPy cauliflower-like morphology composed by small and compact grains is observed for all PPy films (Fig. 5a) [77]. No differences in morphology were observed in terms of the substrate's porosities.

The composite coatings (Fig. 5 b to d) present a similar rough morphology decorated with the silver NPs, the arrows in Fig. 5 mark as an example some of the NPs clusters either in the cross section image of Fig. 5b) or on the surface of the composite that can be better appreciated in the backscattered electron image of Fig. 5c. Higher magnification micrographs in Fig. 5c allow to observe in more detail the presence of the nanoparticles forming small clusters with average, corresponding to association of some nanoparticles according to the UV data of particle size.

SEM cross-sectional images, as in Fig. 5b), were used to measure the thickness of the PPy and PPy-AgNPs composite coatings. An average value from 10 μm to 16 μm was obtained for all coatings, showing similar electropolymerization and film formation for all PPy coatings on the porous substrates. Also, the homogeneous distribution of the Ag NPs all over the thickness of the coating can be observed.

The topography of the PPy coatings was investigated by AFM for coatings deposited over forging and 30 vol % porous substrates (Fig. 6). In both cases, a uniform, granular structure with different grain size is observed. No significant differences are appreciated between both surfaces, indicating that the pores of the porous 30 vol.% substrate are completely covered by the polymeric coating. The AFM-3D scans show the granular structure consistent with the cauliflower morphology observed by the SEM. A higher surface roughness coating is however observed for those deposited on the porous substrates, Sa = 53.35, while for the fully dense forged Ti substrate, the Sa value is much lower, 31.7. As discussed previously, a higher roughness coating could contribute to improve the biocompatibility of the implants.

In the case of the PPy-AgNPs coatings, similar topographic features were observed as expected from the SEM micrographs. These results confirm that the silver NPs are not only on the coatings' surface but well dispersed in all the coating thickness, as previously reported for moderate amounts of AgNPs in PPy [78]. Also, in the

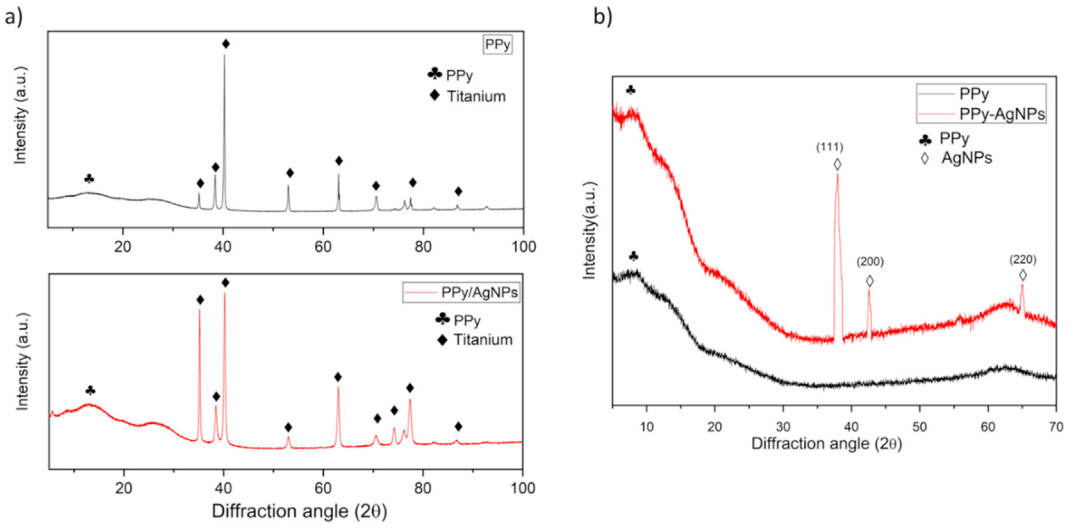

Fig. 4. X-ray diffractograms of polypyrrole (PPy) and PPy-AgNPs coatings: (a) over forged Ti substrate and (b) on self-supported form.

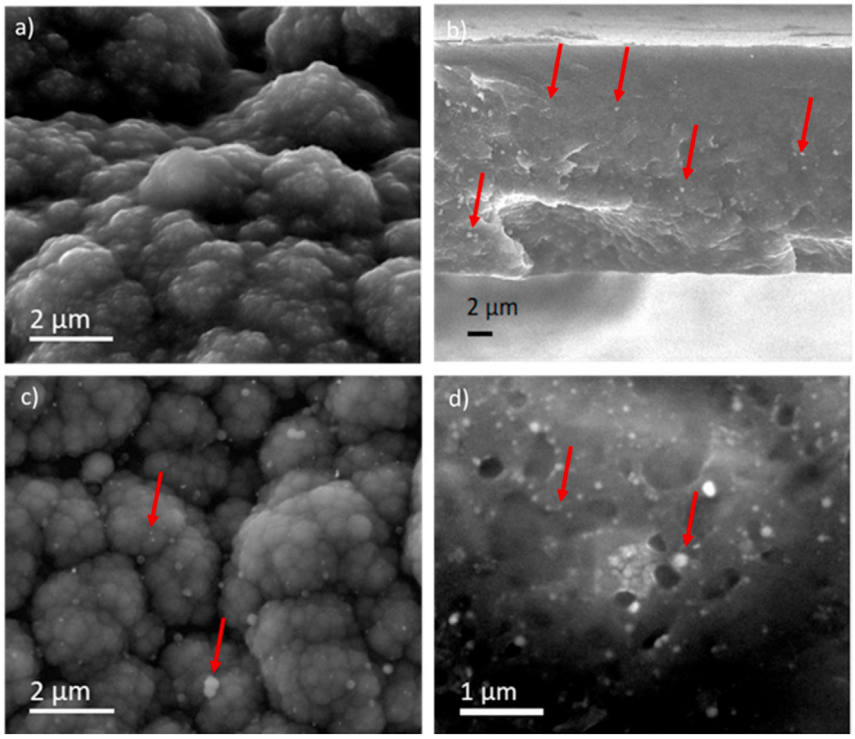

Fig. 5. Scanning electron micrographs showing the cauliflower morphology of polypyrrole (PPy) coating: (a) secondary electrons, PPy/AgNps composite: secondary electrons (b) cross-sectional view showing thickness of the coating (c) surface morphology and (d) backscattered electron image of the coating surface. The arrows point silver NPs clusters.

PPy-AgNPs coatings, a higher roughness is observed for the coatings prepared on the porous substrates, Sa = 77.30 for 30 vol.% while for forged substrates Sa = 39.54. These values are higher compared to the PPy coatings. However, the results point that the nanoparticles are disperse in the coating thickness.

A crucial parameter for the use of the coated supports as implants is the adhesion of the coatings to the substrates. The adhesion of the PPy films was evaluated following the ASTM D4541-02 standard procedure by measuring the minimum pull-off strength to detach the coating in a direction perpendicular to the substrate. The test determines the greatest perpendicular force (in tension) that a surface area can bear before a plug of material is detached. Table 2 displays the adhesion strength values obtained for the different coatings deposited on the different substrates. PPy coatings present an adhesion strength in of about 1 MPa in average, presenting the lowest adhesion strength 0.85 MPa for the PPy coatings deposited on fully dense substrates, and the highest values of 1.3 MPa for the coatings deposited on 30 vol.% and 40%vol. substrates. The adhesion strength of the composite PPy-AgNPs coatings is higher than that of the PPy coatings. The inclusion of Ag NPs forming the composite increases the adhesion of the coatings to the porous substrates to 1.7 MPa. The results in Table 2 point

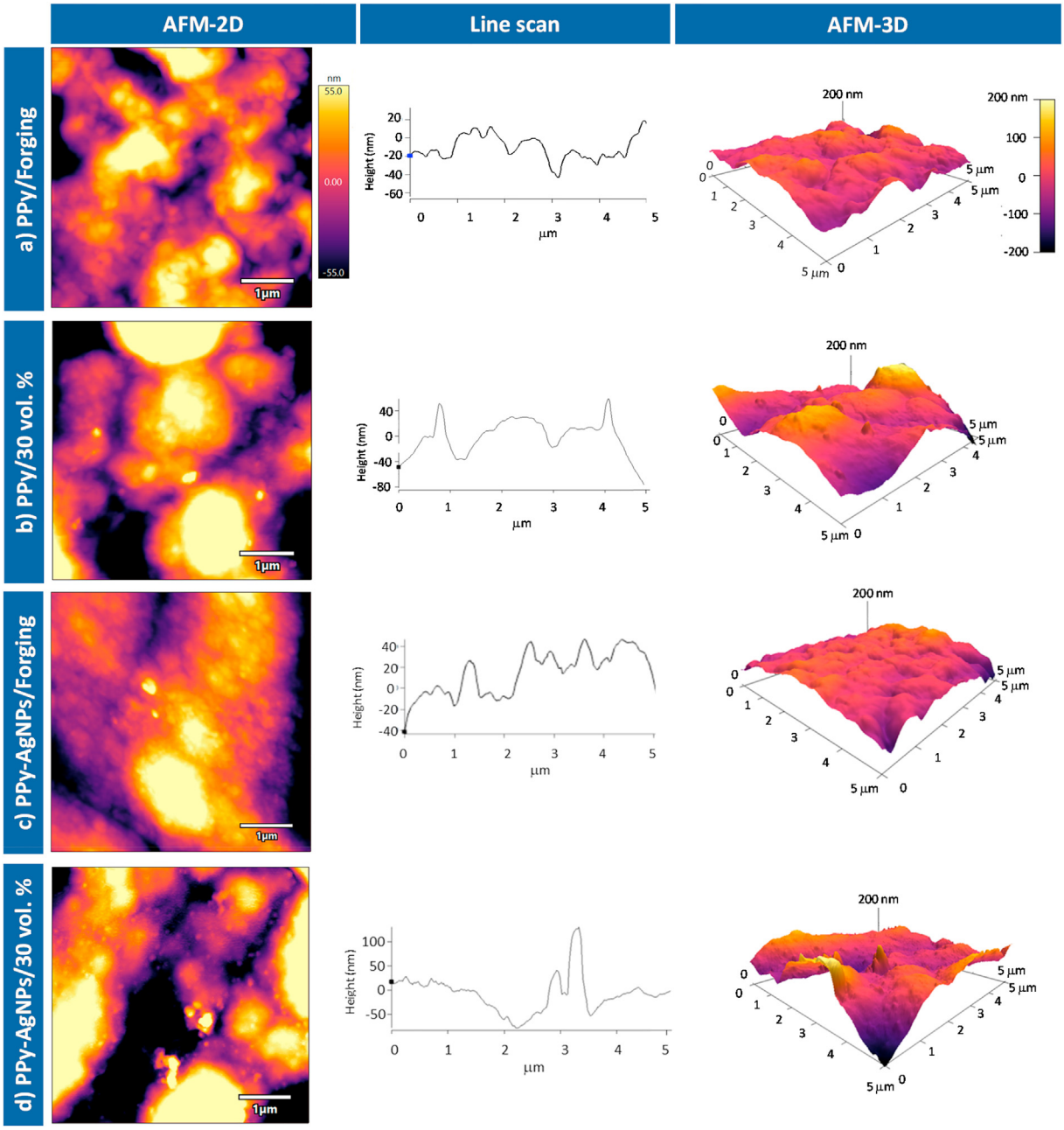

Fig. 6. Atomic force microscopy, 2D maps, line scans, and 3D images of polypyrrole (PPy) and PPy-AgNPs over forging, and 30 vol.% substrates.

Table 2
Adhesion strength, Vickers microhardness, and conductivity of the PPy and PPy-AgNPs coatings over the different substrates.

Sample		Coating	σ adhesion (MPa)]	Hardness (HV)	Conductivity 10^{-4} (S cm^{-1})
Forging		PPy	0.8 ± 0.1	360 ± 4	1.4 ± 0.1
		PPy-AgNPs	1.0 ± 0.1	365 ± 5	12.0 ± 0.7
PM		PPy	1.0 ± 0.1	349 ± 4	1.4 ± 0.1
		PPy-AgNPs	1.2 ± 0.1	355 ± 3	11.7 ± 0.9
SH	30 vol.%	PPy	1.3 ± 0.1	342 ± 5	1.4 ± 0.1
		PPy-AgNPs	1.7 ± 0.1	335 ± 5	12.1 ± 0.8
	40 vol.%	PPy	1.3 ± 0.1	328 ± 3	1.4 ± 0.1
		PPy-AgNPs	1.7 ± 0.13	317 ± 4	12.5 ± 0.9
	50 vol.%	PPy	1.2 ± 0.1	310 ± 3	1.5 ± 0.1
		PPy-AgNPs	1.6 ± 0.1	308 ± 3	11.9 ± 0.7
	60 vol.%	PPy	1.2 ± 0.1	300 ± 3	1.4 ± 0.1
		PPy-AgNPs	1.5 ± 0.1	304 ± 4	12.2 ± 0.8

out two main features, by one hand better adhesion of the polymeric coatings to porous substrates and by the other hand the formation of the composite coatings by the introduction of AgNPs favors the adhesion of the coatings to the substrates. The results allow us to conclude that by electropolymerization, using the 'trapping method', it is possible to form the nanocomposite coatings, giving raise to completely covered substrates with a high surface/volume ratio. These materials could also find application in other fields as sensoring.

Microhardness tests were performed to evaluate the mechanical properties of the coated substrates as a way to provide information on the resistance to load bearing under stress condition. The values in Table 2 correspond to the average values over ten measures. As expected, an increase in the porosity of the substrates has a strong effect on the hardness of the coated substrates [17]. However, coated substrates present higher hardness values compared to bare substrates. The hardness of forged bare Ti substrate is of 284.3 ± 3.7 HV that increases to 360.3 ± 3.8 HV when it is coated by PPy. Coated highly porous 60 vol % Ti substrate presents a hardness 300.4 ± 3.7 HV that is higher than the value presented by the dense cold rolled forged Ti. The increase of hardness by coating with polymeric coatings was previously observed for the case of fully dense Ti coated with chitosan and also reported for stainless-steel substrates coated with PPy [79].

As reported in Table 2 at high loads, no significant differences in hardness were appreciated for the coated substrates between PPy and PPy-AgNPs composite coatings. Nevertheless, microhardness measurements at very low loads of 0.05 Kg, to minimize the effect of the substrate, could indicate a previously reported trend of hardness increase due to the introduction of NPs [26,79]: 195 ± 21 MPa for the PPy coating and 251 ± 39 MPa para PPy-AgNPs for the coating deposited on 30 vol.% substrate. This increase in hardness is associated with a higher density of the coating due to the introduction of a more compact material to the porous PPy and also to a higher roughness presented by the composite coatings.

The hardness values presented by the coated substrates are however similar to previous reported [80] and are in the desired range (250HV-750HV) for biomedical applications in corrosive media.

Table 2 displays also the measured electrical conductivity of the coatings over the Ti substrates. An increase of PPy coating conductivity is associated with an increase of the corrosion protection provided [81]. Several works [82,83] prove that the increase in electrical conductivity can influence the corrosion resistance, to a higher conductivity corresponds a more compact structure which provides a higher corrosion resistance. First, the conductivity of the substrates was evaluated under the same measuring conditions to compare with the substrates. Very low values of 0.57 ± 0.1 Scm^{-1} for forging, 0.58 ± 0.1 Scm^{-1} for PM and 0.60 ± 0.1 Scm^{-1} for 30 vol.% substrates were obtained. In the case of the highly porous Ti substrates, the values were below the sensitivity of the instrument; nevertheless, it should be expected lower values as the density of the substrates is reduced. The PPy conductivity values obtained are in good agreement with published results for coatings [84]. PPy is a semiconductor polymer and its conductivity can be changed by the addiction of dopants; in this work, we used DBSA as dopant that allows for a higher conductivity of PPy [85,86]. As expected, no significant differences were observed among the coatings deposited on the different substrates. The introduction of silver strongly affects the conductivity of the coatings [87], modifying the electronic structure of PPy by displacing the bang [88]. The results show an important increase, one order of magnitude of the electrical conductivity for the composite coatings, with similar results independently of the substrate porosity. According to Sultan et al. [89] silver NPs facilitate a conduction path with low-contact resistance for 'interchain charge transfer'.

3.3. Corrosion behavior

One of the main aims of this work is to determine the effect of PPy and PPy-AgNPs coatings on the corrosion behavior of the Ti substrates as a function of its porosity degree. For that purpose, open circuit potential and AP tests were performed.

The evolution of open circuit potential (OCP) with time allows to characterize the degree of protection that the coatings provide. All coatings were tested in PBS for 3600s comparing the results of coated and bare substrates under the same conditions. Representative results are presented in Fig. 7 for fully dense and 50%vol. substrates. The bare substrates' potential increases over the first periods of the test until it reaches a stable value; this is most probably due to the formation of a stable passive film on the surface of the titanium substrates. When this substrate is coated with PPy and PPy-AgNPs polymeric coatings, there is a decrease of the OCP potentials at the beginning of the tests until it reaches an equilibrium potential that is stable up to the end of the test. Similar behavior has been previously described for dense titanium substrates covered with PPy-based coatings [70].

Fig. 8 resumes the displacement of the OCP potentials (values taken at the end of the OCP) to more positive values for all substrates, independently of its porosity degree, when the different protective coatings are applied. In all cases, coated samples present more positive potentials compared to the bare substrates, which suggests an anodic protection is provided by the coatings. This effect is more significant in the case of the porous titanium substrates, an effective passivation of the metallic substrate either by the formation of an oxide protective layer between the polymeric coating and the Ti substrate or by the diffusion of ions trough the porous polymeric coating [90,91]. Nevertheless, the end potential is dependent on the substrate structure, more negative potentials were found for the samples prepared with higher fraction of SH (50 vol.% y 60 vol.%) with and without protective polymeric PPy-based coating. It is also clear from Figs. 7 and 8, from a thermodynamic point of view, that protective role of PPy-AgNPs coatings is more effective compared to PPy coating.

The displacement to more positive potential provided by the PPy-based coatings was previously reported for other materials as carbon steel [13], stainless steels [25], magnesium [92], titanium [93], and so on. Different mechanisms were proposed to explain this behavior; the most accepted is based on the anodic protection, the polymer acts both as electron transfer medium and as catalyst to the oxygen reduction reaction [94,95]. Other hypothesis is based on the inhibitor effect of the anions released during the polymeric reduction reaction [96,97]. The displacement to more noble potentials when Ag NPs are incorporated to the coating is explained by the enhancement in the electronic transfer due to Ag NPs [50]. Fig. 9 presents a scheme on the proposed anodic protection mechanism, based on reference [12]. The scheme represents the formation of the metal oxide layer that is protecting all surfaces in contact with the electrolyte, including the inner part of accessible pores.

The electrochemical corrosion behavior of coated and uncoated substrates was evaluated using potentiodynamic polarization technique. Fig. 10 shows the representative results for bare and coated forging and porous 30 vol.% Ti substrates (the rest of the samples presented similar curves). In the case of the bare substrates, a wide dissolution zone is observed until a very stable passive titanium oxide layer is formed. In the case of PPy-coated samples, the polarization curves change shape, as expected, since in this case, different phenomena are present: by one hand, the anodic dissolution of the material and also the redox processes taking place at the polymer. Considering that these redox processes are similar in all samples, the potentiodynamic tests can be used in

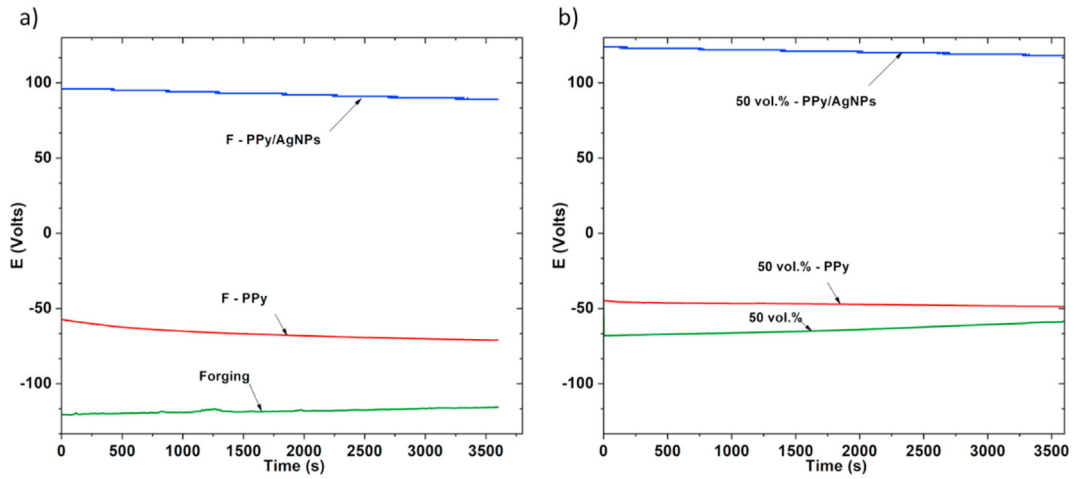

Fig. 7. Open circuit potential evolution of the different coatings over fully dense and 50 vol.% substrates compared to the bare forging substrates.

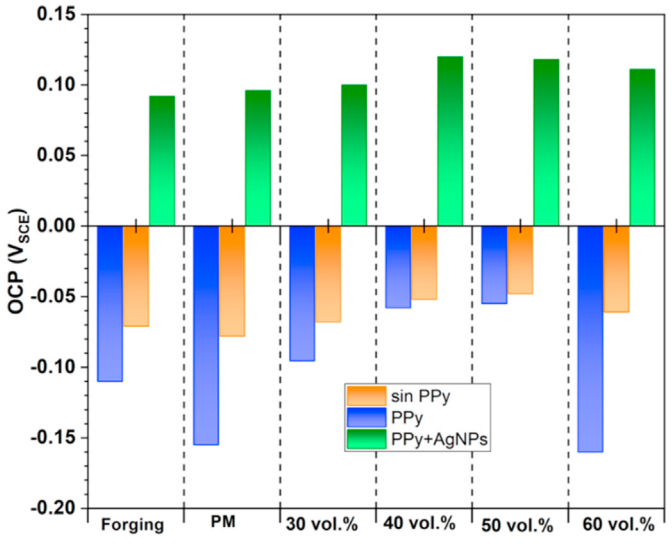

Fig. 8. Comparison of open circuit potential values for the different substrates as function of its porosity and protective polypyrrole-based coatings.

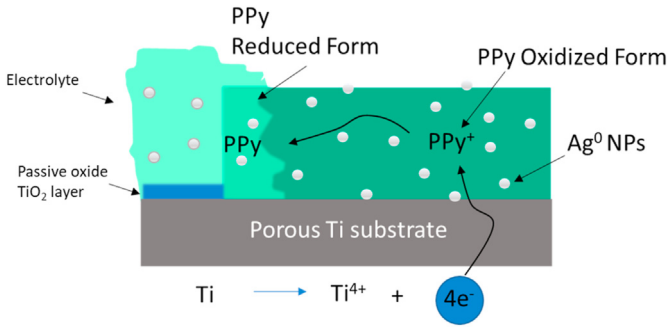

Fig. 9. Anodic protection mechanism, based on reference [12].

a qualitative way to compare the effects of the porosity of the substrates and the addition the silver nanoparticles to the polymeric coating. For coated samples, a lower current density is observed during the major part of the anodic branch; however, the passivation is less stable, and an increase in current at potentials around 0.9 V is observed. In any case, for the aimed applications, this passivation behavior is enough taking into consideration the redox conditions in the human body [98]. In the case of the composite PPy-AgNPs coatings, a strong displacement to more noble potentials and lower current densities is observed indicating a better passive behavior.

Tafel analysis was used to obtain the corrosion parameters such as E_{corr} (corrosion potential), I_{corr} (current density), and R_p (polarization resistance) values were calculated by the Stern–Geary equation, and the results are presented in Table 3. (All tests were repeated three times for each condition and no significant differences between results were observed. The coefficients of variation between these tests are less than 5% for the different methods used.)

To mention the high displacement of the E_{corr} values when the protective composite PPy-AgNPs coatings cover the Ti substrates, these results are in accordance with the OCP results. However, the calculated values of the corrosion potentials are smaller than those corresponding to OCP; the variation is probably due to depassivation phenomenon of the surface during cathodic scanning [99]. Nevertheless, the effect of substrate porosity is similar in both parameters. The highest current density values are achieved for the PM substrates (0 vol.%). It would be expected that as a consequence of a higher surface exposed to the test media, the porous samples should present higher current density values (note that the current density is referred to the geometrical section of the substrate and does not consider the real surface exposed to the electrolyte). This is so in the case of the porous substrates for the increasing porosity, but in the case of the PM substrates, the effect of porosity is more complex. The high values of I_{corr} may be related with a higher percentage of closed pores, originating a higher susceptibility to localized corrosion. The polarization resistance increases when the PPy protective coatings are deposited on the different substrates, being more significant in the case of the PM substrate that presents a very low R_p values without coating. The incorporation of the Ag NPS to the PPy coatings results in a decrease of the current density and increases the polarization resistance for all types of substrates and porosity. Nevertheless, it is worth to mention that the R_p values are in the order of 10^6 Ω/cm^2 for PM (0 vol.%), 30 vol.%, and 40 vol.% substrates, which indicates a high resistance to corrosion [100]. Only in the case of the highly porous substrates, lower R_p values are observed. The composite coatings showed higher R_p values and therefore present higher corrosion resistance compared to the PPy coatings. This increase in the polarization resistance is most

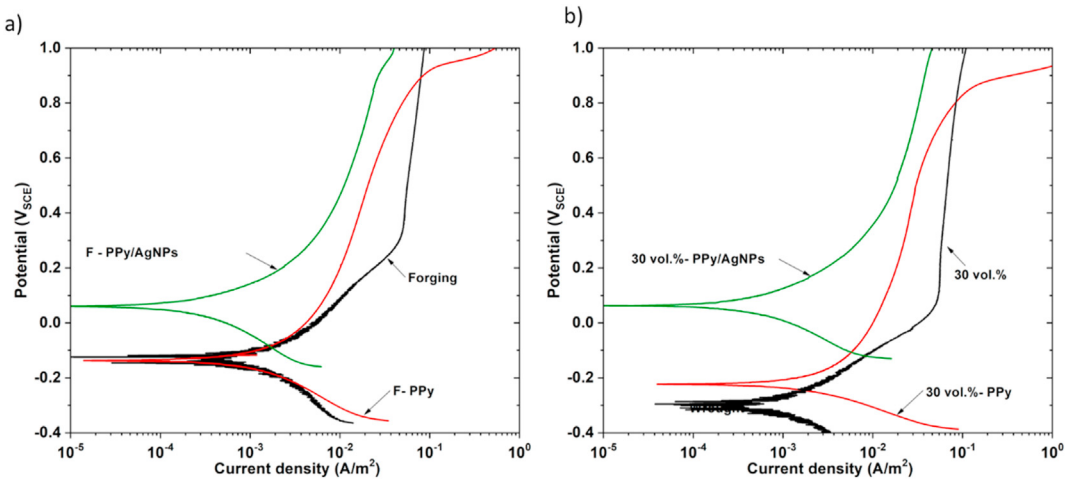

Fig. 10. Potentiodynamic polarization curves in PBS solution of coated and bare: (a) forged, (b) 30 vol.% titanium substrates.

Table 3
Corrosion potential and current density of titanium substrates with and without coatings.

Samples		Coating	E_{corr} (mV)	I_{corr} (μA/cm^2)	R_p (MΩ/cm^2)	PE (%)
Forging		bare	−134 ± 11	0.24 ± 0.02	0.28 ± 0.02	–
		PPy	−137 ± 10	0.09 ± 0.01	0.30 ± 0.03	6.7
		PPy/AgNPs	60 ± 4	0.02 ± 0.01	1.47 ± 0.16	81.6
PM		bare	−168 ± 9	1.32 ± 0.11	0.10 ± 0.01	–
		PPy	−172 ± 12	0.94 ± 0.06	0.51 ± 0.05	80.4
		PPy/AgNPs	73 ± 6	0.12 ± 0.01	2.07 ± 0.27	75.4
SH	30% vol.	bare	−275 ± 12	0.27 ± 0.02	0.17 ± 0.02	–
		PPy	−223 ± 10	0.04 ± 0.01	0.19 ± 0.02	10.5
		PPy/AgNPs	64 ± 6	0.03 ± 0.01	0.65 ± 0.05	73.8
	40% vol.	bare	−253 ± 10	0.71 ± 0.05	0.07 ± 0.01	–
		PPy	−122 ± 9	0.09 ± 0.01	0.25 ± 0.02	72.0
		PPy/AgNPs	48 ± 4	0.06 ± 0.01	0.64 ± 0.06	89.0
	50% vol.	bare	−232 ± 11	0.78 ± 0.08	0.07 ± 0.01	–
		PPy	−129 ± 5	0.41 ± 0.05	0.08 ± 0.01	12.5
		PPy/AgNPs	120 ± 8	0.45 ± 0.04	0.08 ± 0.01	12.5
	60% vol.	bare	−255 ± 12	0.85 ± 0.08	0.05 ± 0.01	–
		PPy	−127 ± 6	0.66 ± 0.07	0.06 ± 0.01	16.7
		PPy/AgNPs	59 ± 4	0.45 ± 0.04	0.07 ± 0.01	28.6

probably due to the formation of an effective barrier against the diffusion of the aggressive ions from the electrolyte, increasing the protection of titanium to the attack of the medium anions. The protection efficiency of the coatings was calculated from equation:

$$PE\ (\%) = [R_p(\text{coating})\text{-}R_p(\text{Ti})] \times 100/R_p(\text{coating}) \quad (1)$$

where PE is the protection efficiency of the coatings, R_p (Ti) is the polarization resistance of the Ti substrates, and R_p (coating) is the polarization resistance of the coated substrates. The protection efficiency increases with the application of the PPy and PPy-AgNPs coatings to all substrates, except in the case of the substrates with the highest volume fraction. This suggests that in the case of these substrates, the formed coatings are not completely continuous or adherent to the substrate decrease its protection.

To understand the effect of the PPy coating, one should take into consideration that during the test, two simultaneous effects are observed: the redox behavior of the polymer and the corrosion resistance [101–103], this explains the changes in the morphology of the AP curves. Other works report the beneficial effect of PPy coatings on the corrosion resistance of different substrates as function of (a) barrier effect [104]; (b) its conductivity (the presence of conjugated double-bonds promotes the electronic transfer that promotes the oxidation of the substrate and its anodic protection) [105]; (c) its effect as catalyst on the oxygen reduction [94,95] and (d) the presence of surfactants as DBSA that can be released and act as inhibitor [25]. Nevertheless, the low effect of PPy on the corrosion resistance of the highly porous substrates reported in this work was also previously observed by other authors on different nonporous metallic substrates [80,92,93] and is explained by one hand by the poor adhesion of PPy to these substrates and on the other hand by the porous nature of PPy that allows for the diffusion of aggressive ions from the electrolyte (chloride ions with small size diffuse easily) that arrive to the interface metal-polymer and could result in galvanic corrosion [106]. Recent studies [107] have also demonstrated that the release of big ions as in the case of DBSA is difficult, so the inhibitor effect is reduced; the movement and the absorption of cations is an easier process that hinders the passivation of the metal substrate.

The higher resistance of the PPy-AgNPs composite coating is explained based on the fact that it is a more compact coating, presenting higher conductivity and also better mechanical properties. Several works have demonstrated the effects of depositing silver on PPy both on the corrosion resistance and antibacterial properties of NiTi substrates [93], magnesium [92] and carbon steels [13,24]. The improvement on the corrosion resistance is

associated with filling the pores of the PPy and with the increase of conductivity. The electrical conductivity has a strong effect on the corrosion properties of polymers [82,83], a more open structure gives raise to lower conductivity values promoting less protection against corrosion. In our work, the silver is introduced not as a layer on top of the coating, but as NPs that are dispersed inside the coating and that were incorporated during the electropolymerization process. Regarding the conjugated polymers of PPy and AgNPs, Chang et al. [108] concluded that these composites have unique physicochemical properties with several potential applications (microelectronics, sensors, energy devices) due to the fact that PPy allows to retain the morphology and colloidal stability of the nanoparticles and at the same time avoids the corrosion of silver. The displacement of the OCP and the E_{corr} to more noble values, together with the decrease of current density observed, shows that the higher conductivity of the PPy-AgNPs coating has a positive effect on the anticorrosion behavior for both dense and porous materials. This positive effect is explained taking into consideration that corrosion involves two processes, on one hand the electronic transfer at the interface metal-electrolyte and on the other hand the diffusion of aggressive ions and corrosion products close to the electrode. The higher conductivity of the composite coatings, due to the presence of the Ag NPs, improves the electronic transfer and allows to form a more stable passivation layer thanks to the anodic protection. On the other hand, the more compact and rough coating will decrease the current that controls the mass transfer. Additionally, it has been demonstrated that the silver NPS improve the corrosion resistance due to its inhibitor effect [109].

Moreover, we compared the anodic behavior of the PPy composite coatings with our previous work with Chitosan-silver composites [6]. Fig. 11 presents for forged and 30 vol.% substrates the comparative results of bare versus coated substrates showing the effect of polymeric coatings and the one of the nanocomposites.

As it can be observed, although the morphology of the curves is different, and characteristic of each polymer, both coatings have a positive effect on the corrosion resistance. Similarly, to what previously discussed for PPy-AgNPs composite coatings, when Ag-NPs are added to Chitosan, an important displacement to more noble potentials is observed both on forged (−230 mV for CS and −112 mV CS-AgNPs coatings respectively) and 30%vol. Substrates (−172 mV for CS and −112 CS-AgNPs coating) together with a reduction of the corrosion current density (on forged substrates from 0.013 μA/cm2 for CS coating to 0.008 μA/cm2 for CS-AgNPs composite coating, on 30%vol. Substrate from 0.018μA/cm2 for CS coating to 0.009μA/cm2 for CS-AgNPs coating) [6].

Nevertheless, important differences can be pointed out between both composite coatings. From the thermodynamic point of view, the PPy-AgNPs composite gives origin to a displacement to more noble potentials compared to the CS-AgNPs. While from a kinetic point of view, the CS-AgNPs coating shows a significant improvement on the corrosion current density with lower passivation current and a more stable passivation layer. Although it is worth mentioning that the main conception idea behind the present work and reference 6 is different (in particular considering that chitosan is a biodegradable polymer), there is a complementary corrosion protection behavior of these two polymers and future work on composite coatings combining both polymers and AgNPs is under consideration.

3.4. Immersion tests

The Ti substrates covered with PPy-AgNPs and with improved corrosion resistance were then submitted to immersion tests over 90 days on PBS solution to determine its ability to form a HA layer on its surface. The formation of the HA layer on the implant surface is a requirement for osseointegration between the living bone tissue and the implant.

After the test, all samples presented a white HA layer of considerable thickness, in the form of scales. The SEM-EDX analysis (Fig. 12 a and b) indicated the presence of Ca and P the semi-quantitative analysis indicates that these elements are present with a ratio Ca/P of 1.62, typical of HA formation. This was confirmed by XRD. Fig. 11 c shows the diffraction pattern of the sample after the immersion test. Apart from the Ti peaks, the main peaks corresponding to HA were identified. These results show that the PBS solution promotes the formation of HA over the PPy-AgNPs composite coatings. The formation of the HA layer has been reported as a way to predict the in vivo bone bioactivity of implants [110]. According to Kokubo and Tadama [110], the formed HA could assist the formation of the bone and cellular activity. Also, Kumar et al. [111] showed that this HA layer presents a higher osteoconductivity exhibiting higher affinity to the living bone cells and allowing that more osteoblast cells form a new bone tissue.

Polymeric PPy coatings are susceptible of swelling and lixiviation when immersed in aggressive media; this would lead to an important decrease of the coating's corrosion resistance. To

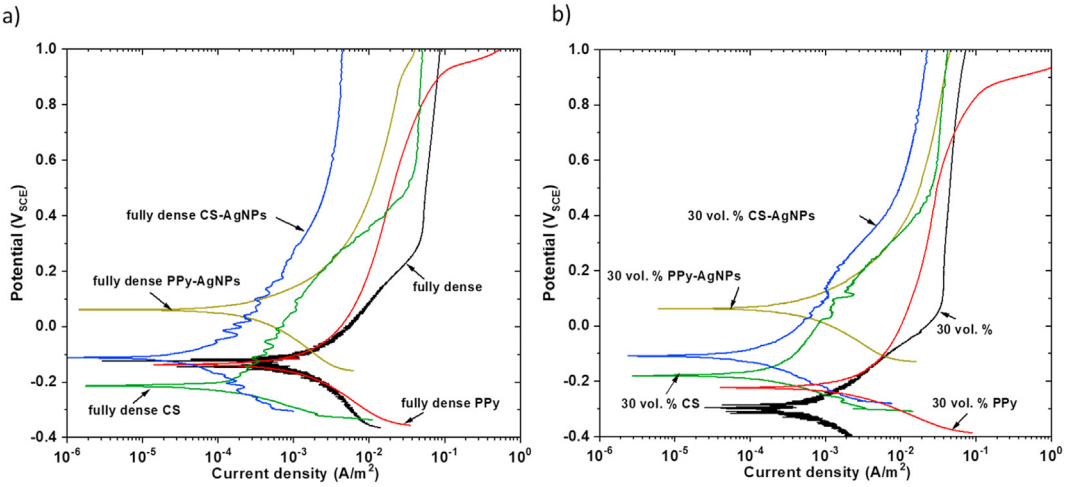

Fig. 11. Effect of the polymeric and composite coatings developed in the present work compared to reference [6] on the potentiodynamic polarization curves for: a) forged, b) 30 vol.% titanium substrates.

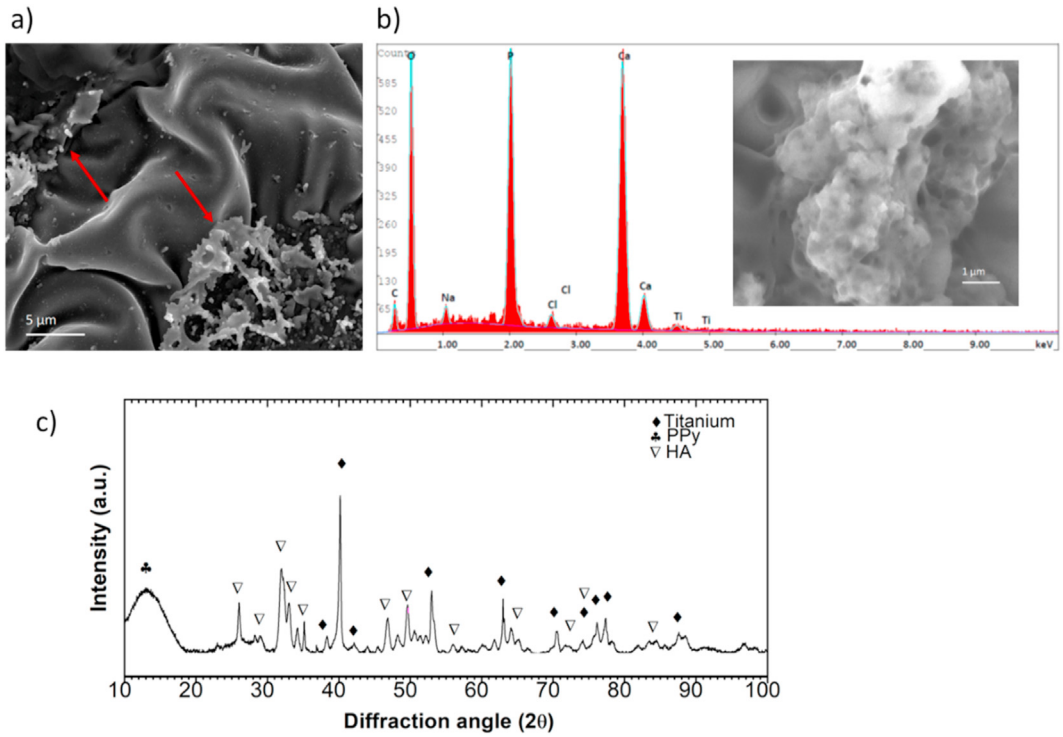

Fig. 12. a) Arrows mark the scales form of hydroxyapatite (HA) layer formed after immersion tests of 90 days in PBS, (b) detail micrograph of HA and respective energy-dispersive X-ray analysis, (c) X-ray diffraction of the sample after 90 days immersion test.

evaluate these possible effects on our coatings, AP tests were performed on the substrates coated with PPy and PPy-AgNPs, after the 90 days' immersion tests in simulated body fluid. Fig. 13 presents the AP curves for coated 30%vol. substrates before and after immersion tests. For both type of coatings, after immersion period, the polarization curves are displaced to more noble potentials, and an important decrease in the current density was observed, indicating that both coatings maintain its protective character after 90 days' immersion in PBS. This behavior agrees with previous results in literature [112,113] in which it is confirmed that apart from a certain tendency to became more porous with immersion time, that would allow the PBS dissolution to further soak the PPy, it also maintains the protection against corrosion.

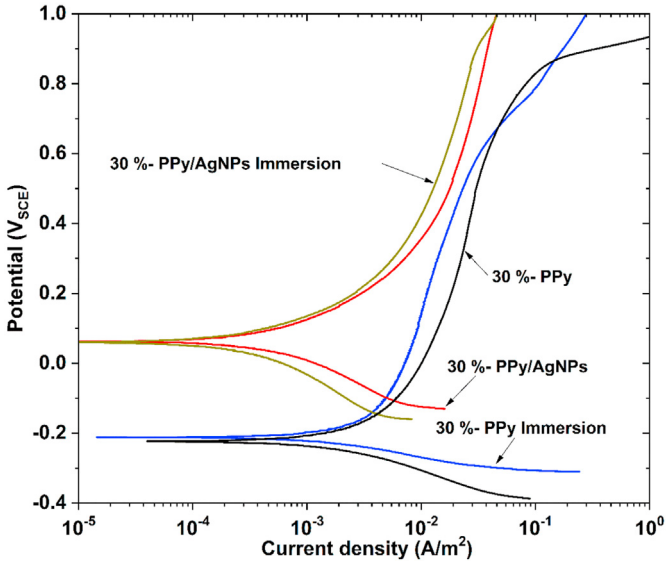

Fig. 13. Anodic polarization curves of coated 30%vol. Ti substrates before and after immersion tests.

EIS measurements were performed to further investigate the long-term corrosion behavior of coated samples. The tests were performed on the coated samples before and after 90 days' immersion tests in simulated body fluid. The impedance data are presented as Nyquist and Bode plots (impedance modulus versus frequency and phase angle versus frequency) in Fig. 14 correspond to the coated 30%vol. substrates. These results are in good correlation to the previously presented, and the nanocomposite coatings show a higher resistance to electronic transfer and a higher impedance modulus, in particular in low frequencies when compared to the PPy-coated samples in both situations, before and after the immersion test.

Regarding the long-term corrosion resistance, the samples coated with PPy present a slight increase in impedance modulus as well as in electronic transfer resistance, indicating a slight increase in the corrosion resistance. In the case of the samples coated with the nanocomposite PPy-AgNPs, its initial good corrosion behavior is maintained after 90 days' immersion test.

ICP tests were also performed to the PBS solution after the 90 days of immersion to evaluate possible dissolution of the metallic titanium, and the obtained results are below 0.1 mg/L, indicating no significant dissolution of the metal.

3.5. Antibacterial activity tests

The antibacterial activity of the coatings was evaluated by the Kirby–Bauer disk diffusion method against *Staphylococcus aureus* (ATCC 25923) as bacterial model. The 30 vol.% coated substrates were used in this test and evaluated against a bare 30 vol.% substrate, used as control, Fig. 15 shows the measurement criteria and

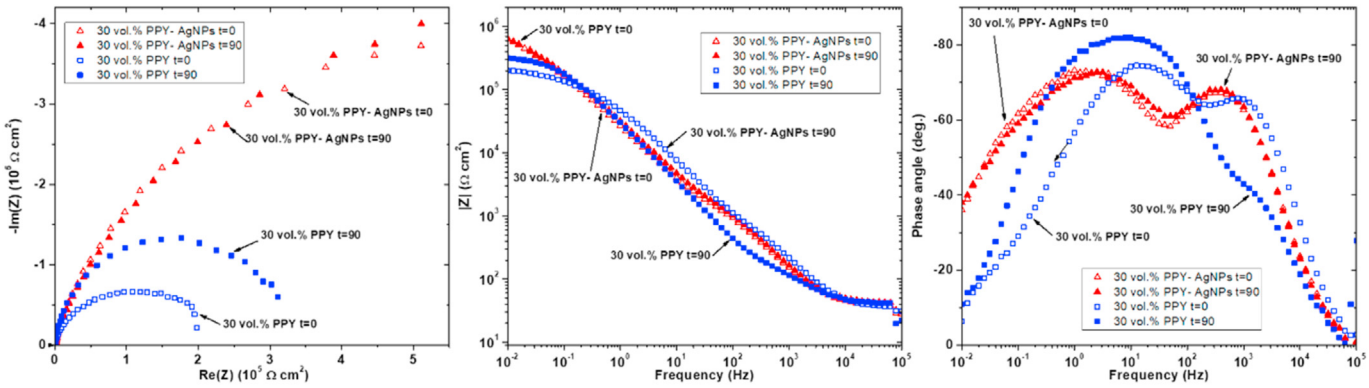

Fig. 14. EIS: (a) Nyquist and (b) and (c) Bode plots o of coated 30%vol. Ti substrates before and after immersion tests.

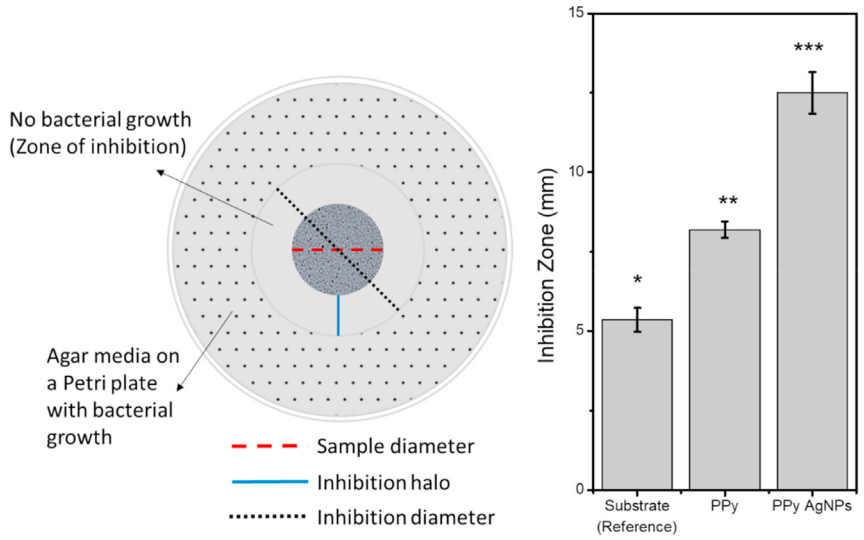

Fig. 15. Inhibition tests results of bare 30 vol.% bare and coated substrates including measurement criteria. Significant differences stand for: * ($p \leq 0.05$), **($p \leq 0.01$), and *** ($p \leq 0.05$).

the obtained results. An inhibition halo of 5.5 ± 0.4 mm was measured for the substrate while PPy and PPy-AgNPs coatings presented a higher halo of 8.2 ± 0.3 and 12.5 ± 0.7 mm, respectively. The antibacterial activity of silver nanoparticles itself is well known [24,109,114,115] as well as in the deposition of silver over PPy [13,92,93].

The mechanism of antibacterial inhibition of PPy coatings has been widely investigated [32] and has been explained based on the electrostatic interactions between the positive charges of the polymer and the negative charges from the cellular membrane of *Staphylococcus aureus* bacteria. Regarding the bacterial inhibition of silver, it has been demonstrated that silver ions bond with the cell modifying its structure and permittivity at the same time that inhibits the protein synthesis and interacts with the nucleic acids leading to cellular death [116,117]. In the case of nanoparticles, its reduced size, electronegativity and high surface/volume ratio promote its permeability in cells and their interaction with enzymes and proteins in the cells [118,119].

4. Conclusions

The present work reports the deposition and characterization of PPy and PPy-AgNPs composite coatings as protective coatings on porous Ti substrates produced by SH technique for small implant applications. The SH prepared Ti materials provide porous substrates with rough surfaces either inner or between pores that improve the adhesion of the electropolymerized coatings. The lack of adhesion of conductive polymers to metallic substrates is one of major drawbacks for its use as protective coatings; the rough surfaces either inner or between pores that improve the adhesion of the electropolymerized coatings. The PPy-Ag NPs composite coatings were prepared just by adding metallic nanoparticles to the electrolyte. The introduction of the Ag NPs improves the mechanical performance and higher adhesion strength of the coatings to the substrates and the conductivity of the coatings one order of magnitude. The conductivity of the PPy and PPy-AgNPs has a strong effect on the corrosion protection of these coatings. The OCP and E_{corr} are displaced to more noble values and a decrease of Icorr is observed, in particular when AgNPs are added to the PPy matrix. The higher conductivity of the composite coatings, due to the presence of the Ag NPS, improves the electronic transfer and allows to form a more stable passivation layer thanks to the anodic protection. Also, more compact coatings are formed in the case of the composite. Immersion tests reveal the formation of a HA layer on the coatings surface after 90 days in PBS. Corrosion tests performed after 90 days in PBS in both PPy and PPy-AgNPs composite coatings indicate that both maintain the protective character after 90 days immersion in PBS.

The coatings proved to have improved antibacterial and cellular activity demonstrated by the presence of HA. This is an innovative strategy that combines two well-known easy and economical preparation techniques, a PM-based SH technique to provide porous Ti substrates with improved biomechanical and bio-functional properties, and electropolymerization to coat these substrates with the PPy-based conductive polymers providing and extra protection against corrosive media being at the same time biocompatible with improved antibacterial activity.

Funding

This work was supported by the Ministry of Science and Innovation of Spain under the grant RTI2018-097990-B-I00 and PID2019-109371 GB-I00, by the Junta de Andalucía−FEDER (Spain) through the Project Ref. US-1259771 and by the Junta de Castilla y Leon (VA275P18 and VA044G19).

Credit author statement

VG, CGC, FMP, and CFG: Writing − original draft preparation, writing − review and editing, CGC, Y, and YT: Conceptualization, methodology, project administration, and funding acquisition. All authors have read and agreed to the published version of the manuscript.

Declaration of competing interest

The authors declare that they have no known competing financial interests or personal relationships that could have appeared to influence the work reported in this paper.

Data availability

Data will be made available on request.

Acknowledgments

The authors would like to dedicate this paper to the memory of Dr. Juan J. Pavón Palacio (University of Antioquia, Colombia).

Appendix A. Supplementary data

Supplementary data to this article can be found online at https://doi.org/10.1016/j.mtchem.2023.101433.

References

[1] Y. Torres, J.J. Pavón, J.A. Rodríguez, Processing and characterization of porous titanium for implants by using NaCl as space holder, J. Mater. Process. Technol. 212 (5) (2012) 1061−1069.
[2] S. Muñoz, J. Pavón, J. Rodríguez-Ortiz, A. Civantos, J. Allain, Y. Torres, On the influence of space holder in the development of porous titanium implants: mechanical, computational and biological evaluation, Mater. Char. 108 (2015) 68−78.
[3] C. Domínguez-Trujillo, A.M. Beltrán, M.D. Garvi, A. Salazar-Moya, J. Lebrato, D.J. Hickey, J.A. Rodríguez-Ortiz, P.H. Kamm, C. Lebrato, F. García-Moreno, Bacterial behavior on coated porous titanium substrates for biomedical applications, Surf. Coating. Technol. 357 (2019) 896−902.
[4] X. Li, X.Y. Ma, Y.F. Feng, Z.S. Ma, J. Wang, T.C. Ma, W. Qi, W. Lei, L. Wang, Osseointegration of chitosan coated porous titanium alloy implant by reactive oxygen species-mediated activation of the PI3K/AKT pathway under diabetic conditions, Biomaterials 36 (2015) 44−54.
[5] N. Eliaz, Corrosion of metallic biomaterials: a review, Materials 12 (3) (2019) 407.
[6] C. García-Cabezón, V. Godinho, C. Salvo-Comino, Y. Torres, F. Martín-Pedrosa, Improved corrosion behavior and biocompatibility of porous titanium samples coated with bioactive chitosan-based nanocomposites, Materials 14 (21) (2021) 6322.
[7] A. Ossowska, A. Zieliński, The mechanisms of degradation of titanium dental implants, Coatings 10 (9) (2020) 836.
[8] S. Cometa, M.A. Bonifacio, M. Mattioli-Belmonte, L. Sabbatini, E. De Giglio, Electrochemical strategies for titanium implant polymeric coatings: the why and how, Coatings 9 (4) (2019) 268.
[9] M. Wang, T. Tang, Surface treatment strategies to combat implant-related infection from the beginning, J Orthopaedic Trans. 17 (2019) 42−54.
[10] N. Kamaly, B. Yameen, J. Wu, O.C. Farokhzad, Degradable controlled-release polymers and polymeric nanoparticles: mechanisms of controlling drug release, Chem. Rev. 116 (4) (2016) 2602−2663.
[11] J. Guo, S. Yuan, W. Jiang, L. Lv, B. Liang, S.O. Pehkonen, Polymers for combating biocorrosion, Frontiers in Mater 5 (10) (2018).
[12] M.K. Zadeh, M. Yeganeh, M.T. Shoushtari, A. Esmaeilkhanian, Corrosion performance of polypyrrole-coated metals: a review of perspectives and recent advances, Synth. Met. 274 (2021), 116723.
[13] A. El Jaouhari, A. El Asbahani, M. Bouabdallaoui, Z. Aouzal, D. Filotás, E.A. Bazzaoui, L. Nagy, G. Nagy, M. Bazzaoui, A. Albourine, D. Hartmann, Corrosion resistance and antibacterial activity of electrosynthesized polypyrrole, Synth. Met. 226 (2017) 15−24.
[14] E. De Giglio, M.R. Guascito, L. Sabbatin, G. Zambonin, Electropolymerization of pyrrole on titanium substrates for the future development of new biocompatible surfaces, Biomaterials 22 (19) (2001) 2609−2616.
[15] S. Cui, J. Mao, M. Rouabhia, S. Elkoun, Z. Zhang, A biocompatible polypyrrole membrane for biomedical applications, RSC Adv. 11 (28) (2021) 16996−17006.
[16] C. Domínguez-Trujillo, E. Peón, E. Chicardi, H. Pérez, J.A. Rodríguez-Ortiz, J.J. Pavón, J. García-Couce, J.C. Galván, F. García-Moreno, Y. Torres, Sol-gel deposition of hydroxyapatite coatings on porous titanium for biomedical applications, Surf. Coating. Technol. 333 (2018) 158−162.
[17] R. Moriche, A.M. Beltrán, B. Begines, J.A. Rodríguez-Ortiz, A. Alcudia, Y. Torres, Influence of the porosity and type of bioglass on the micro-mechanical and bioactive behavior of coated porous titanium substrates, J. Non-Cryst. Solids 551 (2021), 120436.
[18] A. Alcudia, B. Begines, P. Rodriguez-Lejarraga, V. Greyer, V.C.F. Godinho, E. Pajuelo, Y. Torres, Development of porous silver nanoparticle/polycaprolactone/polyvinyl alcohol coatings for prophylaxis in titanium interconnected samples for dental implants, Colloid Interface Sci Commun. 48 (2022), 100621.
[19] Y. Torres, B. Begines, A.M. Beltrán, A.R. Boccaccini, Deposition of bioactive gelatin coatings on porous titanium: influence of processing parameters, size and pore morphology, Surf. Coating. Technol. 421 (2021), 127366.
[20] M. Bazzaoui, J.I. Martins, E.A. Bazzaoui, A. Albourine, L. Martins, Corrosion protection of stainless steel plates in fuel cells environment by conducting polymers, Mater. Corros. 65 (1) (2014) 67−75.
[21] H.N.T. Le, B. Garcia, C. Deslouis, Q. Le Xuan, Corrosion protection and conducting polymers: polypyrrole films on iron, Electrochim. Acta 46 (26−27) (2001) 4259−4272.
[22] K. Aramaki, The healing effect of polymer films containing a non-chromate inhibitor on iron corrosion at scratched surfaces, Corrosion Sci. 42 (11) (2000) 1975−1991.
[23] D. Kowalski, M. Ueda, T. Ohtsuka, Self-healing ion-permselective conducting polymer coating, J. Mater. Chem. 20 (36) (2010) 7630−7633.
[24] K. Jlassi, M.H. Sliem, F.M. Benslimane, N.O. Eltai, A.M. Abdullah, Design of hybrid clay/polypyrrole decorated with silver and zinc oxide nanoparticles for anticorrosive and antibacterial applications, Prog. Org. Coating 149 (2020), 105918.
[25] C. Garcia-Cabezon, C. Garcia-Hernandez, M.L. Rodriguez-Mendez, F. Martin-Pedrosa, A new strategy for corrosion protection of porous stainless steel using polypyrrole films, J. Mater. Sci. Technol. 37 (2020) 85−95.
[26] C. Garcia-Cabezon, C. Salvo-Comino, C. Garcia-Hernandez, M.L. Rodriguez-Mendez, F. Martin-Pedrosa, Nanocomposites of conductive polymers and nanoparticles deposited on porous material as a strategy to improve its corrosion resistance, Surf. Coating. Technol. 403 (2020), 126395.
[27] J.G. de Castro, B.V.M. Rodrigues, R. Ricci, M.M. Costa, A.F.C. Ribeiro, F.R. Marciano, A.O. Lobo, Designing a novel nanocomposite for bone tissue engineering using electrospun conductive PBAT/polypyrrole as a scaffold to direct nanohydroxyapatite electrodeposition, RSC Adv. 6 (39) (2016) 32615−32623.
[28] E.N. Zare, T. Agarwal, A. Zarepour, F. Pinelli, A. Zarrabi, F. Rossi, M. Ashrafizadeh, A. Maleki, M.-A. Shahbazi, T.K. Maiti, R.S. Varma, F.R. Tay, M.R. Hamblin, V. Mattoli, P. Makvandi, Electroconductive multi-functional polypyrrole composites for biomedical applications, Appl. Mater. Today 24 (2021), 101117.
[29] H. Ashassi-Sorkhabi, A. Kazempour, Incorporation of organic/inorganic materials into polypyrrole matrix to reinforce its anticorrosive properties for the protection of steel alloys: a review, J. Mol. Liq. 309 (2020), 113085.
[30] K. Cysewska, L.F. Macía, P. Jasiński, A. Hubin, Tailoring the electrochemical degradation of iron protected with polypyrrole films for biodegradable cardiovascular stents, Electrochim. Acta 245 (2017) 327−336.
[31] S.A.A. Shah, M. Firlak, S.R. Berrow, N.R. Halcovitch, S.J. Baldock, B.M. Yousafzai, R.M. Hathout, J.G. Hardy, Electrochemically enhanced drug delivery using polypyrrole films, Materials 11 (7) (2018) 1123.
[32] F.A.G. da Silva Jr., J.C. Queiroz, E.R. Macedo, A.W.C. Fernandes, N.B. Freire, M.M. da Costa, H.P. de Oliveira, Antibacterial behavior of polypyrrole: the influence of morphology and additives incorporation, Mater. Sci. Eng. C 62 (2016) 317−322.

[33] R. Kumar, M. Oves, T. Almeelbi, N.H. Al-Makishah, M.A. Barakat, Hybrid chitosan/polyaniline-polypyrrole biomaterial for enhanced adsorption and antimicrobial activity, J. Colloid Interface Sci. 490 (2017) 488–496.
[34] M. Maruthapandi, A.P. Nagvenkar, I. Perelshtein, A. Gedanken, Carbon-dot initiated synthesis of polypyrrole and polypyrrole@CuO micro/nanoparticles with enhanced antibacterial activity, ACS Appl. Poly. Mater. 1 (5) (2019) 1181–1186.
[35] Y. Wu, Q. Ruan, C. Huang, Q. Liao, L. Liu, P. Liu, S. Mo, G. Wang, H. Wang, P.K. Chu, Balancing the biocompatibility and bacterial resistance of polypyrrole by optimized silver incorporation, Biomater. Adv. 134 (2022), 112701.
[36] S.B. Ulaeto, G.M. Mathew, J.K. Pancrecious, J.B. Nair, T. Rajan, K.K. Maiti, B. Pai, Biogenic Ag nanoparticles from neem extract: their structural evaluation and antimicrobial effects against Pseudomonas nitroreducens and Aspergillus unguis (NII 08123), ACS Biomater. Sci. Eng. 6 (1) (2019) 235–245.
[37] G. Hu, G. Liang, W. Zhang, W. Jin, Y. Zhang, Q. Chen, Y. Cai, W. Zhang, Silver nanoparticles with low cytotoxicity: controlled synthesis and surface modification with histidine, J. Mater. Sci. 53 (7) (2018) 4768–4780.
[38] J. Gaviria, A. Alcudia, B. Begines, A.M. Beltrán, J.A. Rodríguez-Ortiz, P. Trueba, J. Villarraga, Y. Torres, Biofunctionalization of porous Ti substrates coated with Ag nanoparticles for potential antibacterial behavior, Metals 11 (5) (2021) 692.
[39] T. Jaswal, J. Gupta, A review on the toxicity of silver nanoparticles on human health, Mater. Today Proc. (2021), https://doi.org/10.1016/j.matpr.2021.04.266.
[40] C. Liao, Y. Li, S.C. Tjong, Bactericidal and cytotoxic properties of silver nanoparticles, Int. J. Mol. Sci. 20 (2) (2019) 449.
[41] G.R. Tortella, O. Rubilar, N. Durán, M.C. Diez, M. Martínez, J. Parada, A.B. Seabra, Silver nanoparticles: toxicity in model organisms as an overview of its hazard for human health and the environment, J. Hazard Mater. 390 (2020), 121974.
[42] S.S.D. Kumar, N.K. Rajendran, N.N. Houreld, H. Abrahamse, Recent advances on silver nanoparticle and biopolymer-based biomaterials for wound healing applications, Int. J. Biol. Macromol. 115 (2018) 165–175.
[43] S.P. Deshmukh, S.M. Patil, S.B. Mullani, S.D. Delekar, Silver nanoparticles as an effective disinfectant: a review, Mater. Sci. Eng. C 97 (2019) 954–965.
[44] R.A. Bapat, T.V. Chaubal, C.P. Joshi, P.R. Bapat, H. Choudhury, M. Pandey, B. Gorain, P. Kesharwani, An overview of application of silver nanoparticles for biomaterials in dentistry, Mater. Sci. Eng. C 91 (2018) 881–898.
[45] M. Smekalova, V. Aragon, A. Panacek, R. Prucek, R. Zboril, L. Kvitek, Enhanced antibacterial effect of antibiotics in combination with silver nanoparticles against animal pathogens, Vet. J. 209 (2016) 174–179.
[46] T. Singh, K. Jyoti, A. Patnaik, A. Singh, S.C. Chauhan, Spectroscopic, microscopic characterization of Cannabis sativa leaf extract mediated silver nanoparticles and their synergistic effect with antibiotics against human pathogen, Alex. Eng. J. 57 (4) (2018) 3043–3051.
[47] A. Kaur, S. Preet, V. Kumar, R. Kumar, R. Kumar, Synergetic effect of vancomycin loaded silver nanoparticles for enhanced antibacterial activity, Colloids Surf. B Biointerfaces 176 (2019) 62–69.
[48] B. Aslam, W. Wang, M.I. Arshad, M. Khurshid, S. Muzammil, M.H. Rasool, M.A. Nisar, R.F. Alvi, M.A. Aslam, M.U. Qamar, M.K.F. Salamat, Z. Baloch, Antibiotic resistance: a rundown of a global crisis, Infect. Drug Resist. 11 (2018) 1645–1658.
[49] E.M.d. Araújo Lima, V.N. Holanda, G.P. Ratkovski, W.V.d. Silva, P.H.d. Nascimento, R.C. B.Q.d. Figueiredo, C.P. de Melo, A new biocompatible silver/polypyrrole composite with in vitro antitumor activity, Mater. Sci. Eng. C 128 (2021), 112314.
[50] C. García-Hernández, C. García-Cabezón, C. Medina-Plaza, F. Martín-Pedrosa, Y. Blanco, J.A. de Saja, M.L. Rodríguez-Méndez, Electrochemical behavior of polypyrrol/AuNP composites deposited by different electrochemical methods: sensing properties towards catechol, Beilstein J. Nanotechnol. 6 (1) (2015) 2052–2061.
[51] D. Wang, X. Zhou, R. Song, C. Fang, Z. Wang, C. Wang, Y. Huang, Freestanding silver/polypyrrole composite film for multifunctional sensor with biomimetic micropattern for physiological signals monitoring, Chem. Eng. J. 404 (2021), 126940.
[52] J.J. Pavón, P. Trueba, J.A. Rodríguez-Ortiz, Y. Torres, Development of new titanium implants with longitudinal gradient porosity by space-holder technique, J. Mater. Sci. 50 (18) (2015) 6103–6112.
[53] S. Lascano, C. Arévalo, I. Montealegre-Melendez, S. Muñoz, J.A. Rodriguez-Ortiz, P. Trueba, Y. Torres, Porous titanium for biomedical applications: evaluation of the conventional powder metallurgy frontier and space-holder technique, Appl. Sci. 9 (5) (2019) 982.
[54] P. Trueba, A.M. Beltrán, J.M. Bayo, J.A. Rodríguez-Ortiz, D.F. Larios, E. Alonso, D.C. Dunand, Y. Torres, Porous titanium cylinders obtained by the freeze-casting technique: influence of process parameters on porosity and mechanical behavior, Metals 10 (2) (2020) 188.
[55] J.A. Creighton, C.G. Blatchford, M.G. Albrecht, Plasma resonance enhancement of Raman scattering by pyridine adsorbed on silver or gold sol particles of size comparable to the excitation wavelength, J. Chem. Soc., Faraday Trans. 2: Molecul. Chem. Phys. 75 (1979) 790–798.
[56] A, A. D. t. m., in: A. Method (Ed.), Standard Test Method for Pull-Off Strength of Coatings Using Portable Adhesion Testers, ASTM, West Conshohocken, PA, USA, 1997, 1997.
[57] ASTM Standard G-5-87, ASTM Standard G-5-87, Standard reference test method for Making Potentiostatic and Potentiodynamic Anodic Polarization Measurements, ASTM, Philadelphia, USA, 1993.
[58] A.W. Bauer, W.M.M. Kirby, J.C. Sherris, M. Turck, Antibiotic susceptibility testing by a standardized single disk method, Am. J. Clin. Pathol. 45 (4_ts) (1966) 493–496.
[59] A. Civantos, C. Domínguez, R.J. Pino, G. Setti, J.J. Pavón, E. Martínez-Campos, F.J. Garcia Garcia, J.A. Rodríguez, J.P. Allain, Y. Torres, Designing bioactive porous titanium interfaces to balance mechanical properties and in vitro cells behavior towards increased osseointegration, Surf. Coating. Technol. 368 (2019) 162–174.
[60] A.M. Beltrán, A. Civantos, C. Dominguez-Trujillo, R. Moriche, J.A. Rodríguez-Ortiz, F. García-Moreno, T.J. Webster, P.H. Kamm, A.M. Restrepo, Y. Torres, Porous titanium surfaces to control bacteria growth: mechanical properties and sulfonated polyetheretherketone coatings as antibiofouling approaches, Metals 9 (9) (2019) 995.
[61] F. Rupp, L. Scheideler, D. Rehbein, D. Axmann, J. Geis-Gerstorfer, Roughness induced dynamic changes of wettability of acid etched titanium implant modifications, Biomaterials 25 (7–8) (2004) 1429–1438.
[62] J. Martin, Z. Schwartz, T. Hummert, D. Schraub, J. Simpson, J. Lankford Jr., D. Dean, D. Cochran, B. Boyan, Effect of titanium surface roughness on proliferation, differentiation, and protein synthesis of human osteoblast-like cells (MG63), J. Biomed. Mater. Res. 29 (3) (1995) 389–401.
[63] K. Kieswetter, Z. Schwartz, T. Hummert, D. Cochran, J. Simpson, D. Dean, B. Boyan, Surface roughness modulates the local production of growth factors and cytokines by osteoblast-like MG-63 cells, J. Biomed. Mater. Res.: An Official J Soci. Biomater. Japanese Soc. Biomater. 32 (1) (1996) 55–63.
[64] C. Domínguez-Trujillo, F. Ternero, J.A. Rodríguez-Ortiz, J.J. Pavón, I. Montealegre-Meléndez, C. Arévalo, F. García-Moreno, Y. Torres, Improvement of the balance between a reduced stress shielding and bone ingrowth by bioactive coatings onto porous titanium substrates, Surf. Coating. Technol. 338 (2018) 32–37.
[65] Y. Torres, J.A. Rodríguez, S. Arias, M. Echeverry, S. Robledo, V. Amigo, J.J. Pavón, Processing, characterization and biological testing of porous titanium obtained by space-holder technique, J. Mater. Sci. 47 (18) (2012) 6565–6576.
[66] A. Civantos, M. Giner, P. Trueba, S. Lascano, M.-J. Montoya-García, C. Arévalo, M.Á. Vázquez, J.P. Allain, Y. Torres, In Vitro bone cell behavior on porous titanium samples: influence of porosity by loose sintering and space holder techniques, Metals 10 (5) (2020) 696.
[67] K. Idla, O. Inganäs, M. Strandberg, Good adhesion between chemically oxidised titanium and electrochemically deposited polypyrrole, Electrochim. Acta 45 (13) (2000) 2121–2130.
[68] K. Aoki, I. Mukoyama, J. Chen, Competition between polymerization and dissolution of poly(3-methylthiophene) films, Russ. J. Electrochem. 40 (3) (2004) 280–285.
[69] E. De Giglio, L. De Gennaro, L. Sabbatini, G. Zambonin, Analytical characterization of collagen- and/or hydroxyapatite-modified polypyrrole films electrosynthesized on Ti-substrates for the development of new bioactive surfaces, J. Biomater. Sci. Polym. Ed. 12 (1) (2001) 63–76.
[70] J. Tan, Z. Zhang, D. Ge, Electrodeposition of adherent polypyrrole film on titanium surface with enhanced anti-corrosion performance, MATEC Web Conf 130 (2017), 08007.
[71] W.A. Hammed, M.S. Rahman, H.N.M.E. Mahmud, R. Yahya, K. Sulaiman, Processable dodecylbenzene sulfonic acid (DBSA) doped poly(N-vinyl carbazole)-poly(pyrrole) for optoelectronic applications, Des. Monomers Polym. 20 (1) (2017) 368–377.
[72] S. Shrikrushna, J.A. Kher, M.V. Kulkarni, Influence of dodecylbenzene sulfonic acid doping on structural, morphological, electrical and optical properties on polypyrrole/3C-SiC nanocomposites, J. Nanomed. Nanotechnol. 6 (5) (2015) 1.
[73] Y. Wei, L. Li, X. Yang, G. Pan, G. Yan, X. Yu, One-step UV-induced synthesis of polypyrrole/Ag nanocomposites at the water/ionic liquid interface, Nanoscale Res. Lett. 5 (2) (2009) 433.
[74] T. Yao, C. Wang, J. Wu, Q. Lin, H. Lv, K. Zhang, K. Yu, B. Yang, Preparation of raspberry-like polypyrrole composites with applications in catalysis, J. Colloid Interface Sci. 338 (2) (2009) 573–577.
[75] M.M. Ayad, E. Zaki, Synthesis and characterization of silver–polypyrrole film composite, Appl. Surf. Sci. 256 (3) (2009) 787–791.
[76] Y.M. Mohan, T. Premkumar, K. Lee, K.E. Geckeler, Fabrication of silver nanoparticles in hydrogel networks, Macromol. Rapid Commun. 27 (16) (2006) 1346–1354.
[77] C. Liu, Z. Cai, Y. Zhao, H. Zhao, F. Ge, Potentiostatically synthesized flexible polypyrrole/multi-wall carbon nanotube/cotton fabric electrodes for supercapacitors, Cellulose 23 (1) (2016) 637–648.
[78] M.A. Vorotyntsev, M. Skompska, A. Rajchowska, J. Borysiuk, M. Donten, A new strategy towards electroactive polymer–inorganic nanostructure composites. Silver nanoparticles inside polypyrrole matrix with pendant titanocene dichloride complexes, J. Electroanal. Chem. 662 (1) (2011) 105–115.
[79] A.M. Kumar, N. Rajendran, Electrochemical aspects and in vitro biocompatibility of polypyrrole/TiO2 ceramic nanocomposite coatings on 316L SS for orthopedic implants, Ceram. Int. 39 (5) (2013) 5639–5650.

[80] B. Rikhari, S.P. Mani, N. Rajendran, Electrochemical behavior of polypyrrole/chitosan composite coating on Ti metal for biomedical applications, Carbohydr. Polym. 189 (2018) 126–137.
[81] S. Wan, C.-H. Miao, R.-M. Wang, Z.-F. Zhang, Z.-H. Dong, Enhanced corrosion resistance of copper by synergetic effects of silica and BTA codoped in polypyrrole film, Prog. Org. Coating 129 (2019) 187–198.
[82] A. Olad, M. Barati, H. Shirmohammadi, Conductivity and anticorrosion performance of polyaniline/zinc composites: investigation of zinc particle size and distribution effect, Prog. Org. Coating 72 (4) (2011) 599–604.
[83] I.L. Lehr, S.B. Saidman, Anticorrosive properties of polypyrrole films modified with Zinc onto SAE 4140 steel, Prog. Org. Coating 76 (11) (2013) 1586–1593.
[84] C.C. Manole, F. Maury, I. Demetrescu, Patterned PPy polymer and PPy/Ag nanocomposites thin films by photo-DLICVD, Phys. Procedia 46 (2013) 46–55.
[85] Y. Wang, X. Jing, Intrinsically conducting polymers for electromagnetic interference shielding, Polym. Adv. Technol. 16 (4) (2005) 344–351.
[86] R.A.M. Campos, R. Faez, M.C. Rezende, Synthesis of polypyrrole with anionic surfactants targeting applications such as microwave absorbers, Polímeros 24 (3) (2014) 351–359.
[87] M.H. Abdulmajeed, H.A. Abdullah, S.I. Ibrahim, G.Z. Alsandooq, Investigation of corrosion protection for steel by eco-friendly coating, Eng. Technol. J. 37 (2) (2019) 52–59.
[88] A. Alqudami, S. Annapoorni, P. Sen, R. Rawat, The incorporation of silver nanoparticles into polypyrrole: conductivity changes, Synth. Met. 157 (1) (2007) 53–59.
[89] A. Sultan, F. Mohammad, Chemical sensing, thermal stability, electrochemistry and electrical conductivity of silver nanoparticles decorated and polypyrrole enwrapped boron nitride nanocomposite, Polymer 113 (2017) 221–232.
[90] B.N. Grgur, P. Živković, M.M. Gvozdenović, Kinetics of the mild steel corrosion protection by polypyrrole-oxalate coating in sulfuric acid solution, Prog. Org. Coating 56 (2–3) (2006) 240–247.
[91] M. Bazzaoui, J. Martins, S. Costa, E. Bazzaoui, T. Reis, L. Martins, Sweet aqueous solution for electrochemical synthesis of polypyrrole: Part 2. On ferrous metals, Electrochim. Acta 51 (21) (2006) 4516–4527.
[92] A.D. Forero López, I.L. Lehr, L.I. Brugnoni, S.B. Saidman, Improvement in the corrosion protection and bactericidal properties of AZ91D magnesium alloy coated with a microstructured polypyrrole film, J. Magnes. Alloys 6 (1) (2018) 15–22.
[93] M. Saugo, D.O. Flamini, L.I. Brugnoni, S.B. Saidman, Silver deposition on polypyrrole films electrosynthesised onto Nitinol alloy. Corrosion protection and antibacterial activity, Mater. Sci. Eng. C 56 (2015) 95–103.
[94] T.D. Nguyen, M. Keddam, H. Takenouti, Device to study electrochemistry of iron at a defect of protective coating of electronic conducting polymer, Electrochem. Solid State Lett. 6 (8) (2003) B25.
[95] U. Rammelt, P. Nguyen, W. Plieth, Corrosion protection by ultrathin films of conducting polymers, Electrochim. Acta 48 (9) (2003) 1257–1262.
[96] J.I. Martins, L. Diblikova, M. Bazzaoui, M. Nunes, Polypyrrole coating doped with dihydrogenophosphate ion to protect aluminium against corrosion in sodium chloride medium, J. Braz. Chem. Soc. 23 (3) (2012) 377–384.
[97] N. Hien, B. Garcia, A. Pailleret, C. Deslouis, Role of doping ions in the corrosion protection of iron by polypyrrole films, Electrochim. Acta 50 (7–8) (2005) 1747–1755.
[98] H. Gerengi, A. Jazdzewska, M. Kurtay, A comprehensive evaluation of mimosa extract as a corrosion inhibitor on AA6060 alloy in acid rain solution: part I. Electrochemical AC methods, J. Adhes. Sci. Technol. 29 (1) (2015) 36–48.
[99] R. Noftle, D. Pletcher, The mechanism of electrodeposition of composite polymers including polypyrrole, J. Electroanal. Chem. Interfacial Electrochem. 227 (1–2) (1987) 229–235.
[100] F. Turelli, A.T. Strigin, A.L. Belinkii, N.A. Adugina, M.A. Dmitriev, A.N. Krutikov, Simultaneous determination of instantaneous corrosion rates and tafel slopes from polarization resistance measurements, J. Electrochem. Soc. 120 (4) (1972) 6–9.
[101] M. Arenas, L.G. Bajos, J. De Damborenea, P. Ocón, Synthesis and electrochemical evaluation of polypyrrole coatings electrodeposited onto AA-2024 alloy, Prog. Org. Coating 62 (1) (2008) 79–86.
[102] D.O. Flamini, S.B. Saidman, Electrodeposition of polypyrrole onto NiTi and the corrosion behaviour of the coated alloy, Corrosion Sci. 52 (1) (2010) 229–234.
[103] V. Annibaldi, A.D. Rooney, C.B. Breslin, Corrosion protection of copper using polypyrrole electrosynthesised from a salicylate solution, Corrosion Sci. 59 (2012) 179–185.
[104] B. Rikhari, S.P. Mani, N. Rajendran, Investigation of corrosion behavior of polypyrrole-coated Ti using dynamic electrochemical impedance spectroscopy (DEIS), RSC Adv. 6 (83) (2016) 80275–80285.
[105] S. Biallozor, A. Kupniewska, Conducting polymers electrodeposited on active metals, Synth. Met. 155 (3) (2005) 443–449.
[106] K. Qi, Y. Qiu, Z. Chen, X. Guo, Corrosion of conductive polypyrrole: effects of possibly formed galvanic cells, Corrosion Sci. 80 (2014) 318–330.
[107] A. Michalik, M. Rohwerder, Conducting Polymers for Corrosion Protection: a Critical View, 2005.
[108] M. Chang, T. Kim, H.-W. Park, M. Kang, E. Reichmanis, H. Yoon, Imparting chemical stability in nanoparticulate silver via a conjugated polymer casing approach, ACS Appl. Mater. Interfaces 4 (8) (2012) 4357–4365.
[109] E. Ituen, L. Yuanhua, C. Verma, A. Alfantazi, O. Akaranta, E.E. Ebenso, Multifunctional silver nanocomposite: a potential material for antiscaling, antimicrobial and anticorrosive applications, JCIS Open 3 (2021), 100012.
[110] T. Kokubo, H. Takadama, How useful is SBF in predicting in vivo bone bioactivity? Biomaterials 27 (15) (2006) 2907–2915.
[111] A.M. Kumar, S. Nagarajan, S. Ramakrishna, P. Sudhagar, Y.S. Kang, H. Kim, Z.M. Gasem, N. Rajendran, Electrochemical and in vitro bioactivity of polypyrrole/ceramic nanocomposite coatings on 316L SS bio-implants, Mater. Sci. Eng. C 43 (2014) 76–85.
[112] S.A. Pauline, N. Rajendran, Biomimetic novel nanoporous niobium oxide coating for orthopaedic applications, Appl. Surf. Sci. 290 (2014) 448–457.
[113] A.M. Kumar, N. Rajendran, Influence of zirconia nanoparticles on the surface and electrochemical behaviour of polypyrrole nanocomposite coated 316L SS in simulated body fluid, Surf. Coating. Technol. 213 (2012) 155–166.
[114] C. Pragathiswaran, G. Thulasi, M.M. Al-Ansari, L.A. Al-Humaid, M. Saravanan, Experimental investigation and electrochemical characterization of titanium coated nanocomposite materials for biomedical applications, J. Mol. Struct. 1231 (2021), 129932.
[115] H. Huang, L. Mao, Z. Li, Y. Liu, S. Fan, Y. Jin, J. Xie, Multifunctional polypyrrole-silver coated layered double hydroxides embedded into a biodegradable polymer matrix for enhanced antibacterial and gas barrier properties, J. Bioresources Bioproducts 4 (4) (2019) 231–241.
[116] W.K. Jung, H.C. Koo, K.W. Kim, S. Shin, S.H. Kim, Y.H. Park, Antibacterial activity and mechanism of action of the silver ion in Staphylococcus aureus and Escherichia coli, Appl. Environ. Microbiol. 74 (7) (2008) 2171–2178.
[117] Q.L. Feng, J. Wu, G.Q. Chen, F.Z. Cui, T.N. Kim, J.O. Kim, A mechanistic study of the antibacterial effect of silver ions on Escherichia coli and Staphylococcus aureus, J. Biomed. Mater. Res. 52 (4) (2000) 662–668.
[118] E. Ituen, E. Ekemini, L. Yuanhua, R. Li, A. Singh, Mitigation of microbial biodeterioration and acid corrosion of pipework steel using Citrus reticulata peels extract mediated copper nanoparticles composite, Int. Biodeterior. Biodegrad. 149 (2020), 104935.
[119] S. Shaikh, N. Nazam, S.M.D. Rizvi, K. Ahmad, M.H. Baig, E.J. Lee, I. Choi, Mechanistic insights into the antimicrobial actions of metallic nanoparticles and their implications for multidrug resistance, Int. J. Mol. Sci. 20 (10) (2019) 2468.